MEASURE, MODELING AND COMPENSATION OF FATIGUE-INDUCED DELAY DURING NEUROMUSCULAR ELECTRICAL STIMULATION

By

FANNY BOUILLON

A THESIS PRESENTED TO THE GRADUATE SCHOOL
OF THE UNIVERSITY OF FLORIDA IN PARTIAL FULFILLMENT
OF THE REQUIREMENTS FOR THE DEGREE OF
MASTER OF SCIENCE

UNIVERSITY OF FLORIDA

2013

To my grandparents

ACKNOWLEDGMENTS

I would like sincerely to thank the persons who contributed to the success of this project: my advisor at the University of Florida, Dr. Warren Dixon, my advisor at Télécom Physique Strasbourg, Pr. Bernard Bayle, Ryan Downey for his precious help, advice and patience all over the year, Christophe Collet and Shelly Burleson, Lyn Straka and Abigail Nelson, the NCR August 2012/August 2013 group, Dr. Donald Bolser and Dr. Teresa Pitts. Thanks to my parents, sister and brothers for their support through this whole year.

TABLE OF CONTENTS

LIST OF FIGURES

LIST OF TABLES

Abstract of Thesis Presented to the Graduate School
of the University of Florida in Partial Fulfillment of the
Requirements for the Degree of Master of Science

MEASURE, MODELING AND COMPENSATION OF FATIGUE-INDUCED DELAY DURING NEUROMUSCULAR ELECTRICAL STIMULATION

By

Fanny Bouillon

August 2013

Chair: Warren E. Dixon
Major: Mechanical Engineering

Neuromuscular Electrical Stimulation (NMES) is a developing method used for rehabilitation after surgery or for patients suffering from trauma and diseases. Functional Electrical Stimulation (FES) is the specific use of NMES to produce functional tasks, without the intervention of the nervous system. NMES training may be of long duration and NMES may induce muscle fatigue for the patients. The nonlinear response of the muscle is rendered more complex with external factors, including fatigue. Fatigue leads to a decreased muscle force in response to stimulation, and fatigue is suspected to lengthen the time lag from the onset of the electrical stimulus to the response of the muscle, termed electromechanical delay (EMD). Evolution of EMD was investigated on 5 male and 5 female subjects. The subjects' muscles were fatigued through NMES exercises, consisting of constant voltage stimulation applied to the quadriceps femoris muscle group to produce isometric contractions. EMD was measured using monophasic electrical pulse trains of 0.5 seconds, characterized with constant frequency and voltage. Fatigue was induced with pulse trains of the same stimulation frequency and voltage applied over a longer period of time. Force production were measured throughout the trials for all the experiments. Fatigue was quantified by the decrease in force produced by the muscle when stimulated with constant parameters. The results showed an increase of the EMD with fatigue, up to 3 times its initial value. An exponential model was found to fit the evolution of the EMD in terms of fatigue. In order to track a desired

angular position trajectory, a time-varying input delay compensation was designed for nonlinear systems. The fatigue-varying EMD model was implemented in the controller as a time-varying input delay model. Experiments were conducted to determine the performance of the controller and the goodness of the EMD model. The experiments consisted of two sessions separated by several hours.The first session was used as a control test and did not involve any delay compensation. The controller used in the second session included time-varying input delay compensation adapted to NMES. The time-varying delay was compensated based on the estimation provided by the first session. The experiments run with this controller showed promising results, including a decreased delay between the input and the response.

CHAPTER 1
INTRODUCTION

1.1 Context

Neuromuscular electrical stimulation (NMES) is the process of applying an electrical potential across a muscle to yield a muscle contraction. NMES is commonly used for rehabilitation after trauma, surgery, or to treat neuromuscular disorder and disease, such as spinal cord injury (SCI) and Parkinson's disease. NMES can be an alternative method to or complement traditional therapy. NMES can be used to produce functional tasks or movements where it is termed functional electrical stimulation (FES). Traditional NMES-based rehabilitation is to strengthen muscle, whereas more advanced methods focus on closed-loop control of the limbs.

A challenge for these advanced methods is that skeletal muscle has a nonlinear response to an external electrical stimulus. The response depends on various factors related to the condition of the person who is stimulated, the stimulation parameters, and the muscle length and velocity. The onset of muscle fatigue is more rapid during (NMES) than during voluntary contractions [1–3]. The response to stimulation changes as the muscle fatigues [4–6], and thus, premature fatigue may limit the effectiveness of rehabilitation by limiting the duration of the performance of a task. The focus of this thesis is to investigate and compensate for changes in the electromechanical delay (EMD), defined here as the time difference between the onset of the stimulation and the onset of an actual movement of the stimulated limb, in the quadriceps femoris muscle group as a function of fatigue.

1.2 Literature Review

Previous literature has related the dependency of the EMD with muscle type, or stimulation type, but the relationship between the delay and the fatigue state of the muscle during NMES is not clear.

Previous research targets the development of relationships between EMD and the intensity of contractions [7, 8], or the type of exercise (i.e. electrical stimulation versus voluntary contractions) [8]. EMD is also correlated to the maximal voluntary contraction and the torque produced by the muscle. Specifically, the results in [9], indicated that EMD is shorter for individuals who can produce strong maximal voluntary contractions. EMD variations in NMES has also been compared between different aged people [10, 11]. Both of these papers found a significant increased EMD in older subjects. EMD was also compared between men and women, but different results were observed: shorter EMD for men were reported in [12, 13], while the results of [11] indicated a difference of EMD between the two genders only among the 18-24 year old range, and the results in [10] did not show any significant change for the 2 groups within their 30 subjects. EMD has been examined prior to and following a single fatiguing protocol during voluntary [14, 15] and NMES-induced [10] contractions. In 2001, Kubo found an actual decrease of the EMD with fatigue, after the subjects are trained [16].

Significant increases in EMD during voluntary fatiguing exercises were reported in [10, 15, 17, 18], where EMD was measured as the time lag between the onset of electrical activity (measured with electromyography) and the onset of force production. However, to the extent of the authors' knowledge no study has examined or modeled the EMD with respect to NMES-induced fatigue. To provide an indicator of muscle fatigue during isometric contractions, this study will measure the force produced by the muscle in response to both electrical stimulation and voluntary contractions, as in [14, 19–21], through a force transducer.

Few FES closed-loop systems were designed to include an input delay compensation. Studies in [22–25] involved PD controllers, without any EMD prediction term. Moreover, the results presented in those studies are not supported through mathematical proof of stability. The only prior work that accounts for EMD during NMES closed-loop is described in [26]. However, this result assumes a constant input delay.

1.3 Outline

The following study aims to state the relationship between the EMD and the fatigue due to electrical stimulation of the quadriceps femoris muscle group. Fatigue experiments were executed while the time-varying EMD was measured.

Chapter 1 describes the context and state of the art related to understanding EMD during NMES/FES. Only a few results examine the variations of EMD with fatigue. The only prior result that compensates for EMD during closed-loop control, assures the delay is constant. Therefore, this chapter highlights the novelty of the research described in this thesis.

Chapter 2 first presents the methods and technological tools used to run NMES experiments and EMD collect data. This chapter also gathers the results of the evoked experiments and studies the evolution of the EMD with fatigue. The variations of the EMD are analyzed through different mechanical parameters, and a fatigue-varying model for the EMD in terms of force production during isometric contractions is investigated.

Finally Chapter 3 applies a RISE-based NMES controller, that compensate for the time-varying EMD. The time-varying input delay is included in the RISE-based controller through a prediction term. The contributions of a time-varying input delay compensator are then compared with the same controller without the delay prediction.

CHAPTER 2
MODELING FATIGUE-BASED ELECTROMECHANICAL DELAY

2.1 Equipment and Participants

The objective in this chapter is to correlate EMD with the fatigue state of the quadriceps femoris muscle group during isometric contractions. To study the evolution of the EMD, a group of ten volunteer subjects were stimulated to a level of fatigue while EMD was measured. The group was composed of five males and five females, aged 19 to 26. All participants signed an informed consent, approved by the Institutional Review Board of the University of Florida.

Subjects were seated in a leg extension machine (LEM), depicted in Figure 2-1A). The leg extension machine was modified such that the subjects' legs could be securely fixed to the machine. A boot was fixed to the leg extension machine through a force transducer that was used to record the force produced when the muscle was stimulated (see Figure 2-1B)). Stimulation was delivered through a pair of self-adhesive surface electrode pads, placed over the quadriceps femoris muscle group (see Figure 2-2).

Pulse trains used in this study were to 30 Hz monophasic square electrical signals with a constant pulse width of 600 µs. The intersubject voltage amplitude varied from 20 to 40 V depending on each subject's response; however, the voltage amplitude remained constant for each subject.

2.2 Protocol

The objective was to characterized the delayed response of the muscle in terms of fatigue, in healthy individuals. The initial EMD and force production for each subject were recorded from a resting position prior to experimental trials. To measure the EMD, a long stimulation duration is not necessary; thus, short pulse trains lasting 0.5 seconds were used to determine the moment when the muscle started to produce force. To obtain a more accurate measure of EMD, ten short pulse trains were applied, allowing a calculation of a mean value of the delay, immediately following a long stimulation.

The EMD is measured as the time difference between the onset of stimulation and the onset of muscle force production, where the threshold used to characterize the onset of force production was defined as 0.02% of the maximal voluntary contraction the subject performed at the beginning of the experiment (see Figure 2-3). Voluntary contractions were then performed to determine the maximal voluntary contraction (MVC) that the subject can achieve. These preliminary tests were designed such that they would not induce fatigue, and the corresponding measurements were used to normalize the subsequent EMD and force measurements for each subject.

After pretrial tests were completed, trials were performed to fatigue the muscle. Fatigue trials consisted of long pulse trains with constant stimulation parameters lasting 20 to 35 seconds. Once calibrated for the subject, the duration remained constant for all the trials of a given subject. After each fatigue trial, another set of short pulse trains was applied to measure the average of the new state of the muscle in terms of the EMD and force production. Then the subject was asked to perform three maximal contractions. Finally, a longer set of short pulse trains was applied to measure of the evolution of the EMD during recovery. Each trial was repeated at least eight times for each subject. The number of cycles depended on subject comfort and level of fatigue. The duration of stimulation and the voltage applied to fatigue the muscle vary between subjects, but remain the same during all trials for a given subject. The duration varied among the subjects from twenty-five to thirty-five seconds.

2.3 Results

The data gathered during the ten experiments are reported below.

2.3.1 Mechanical Delays

Ten short pulse trains, each separated by one second, were applied to measure the average EMD after fatigue trials. Tables 2-1 and 2-2 report the values of the EMD obtained for each subject following each fatigue trial. Table 2-1 reports the raw values,

expressed in seconds. At the beginning of each trial, the EMD was recorded and used to normalize the subsequent values. These normalized values are reported in Table 2-2. The mean initial value of EMD was 46.8 ms, and ranged from 14 to 105 ms. For 20% of the experiment group, the variation of the EMD stayed between 1 and 1.5 of the initial value. Sixty percent of the subjects exhibited a maximal EMD which was 80% longer than the initial EMD. For 40% of the subjects the maximum is reached after three to eight long stimulation. The results clearly indicate that the EMD varies with fatigue, within a range, and in most cases, remains higher than its initial value until a recovery period.

The next section will further investigate the change of EMD with fatigue.

2.3.2 Force During Stimulation

An extract of a record is depicted in Figure 2-6, reporting the variations of the normalized force production during muscle fatigue for one subject. The horizontal cursors on the figure indicate the important decrease of the force, with the fatigue trials, whereas the level of the voluntary force values remains constant. The peak values of the force elicited from the long pulse trains are reported in Table 2-3 and are plotted in Figure 2-7. This data indicates that 30% of the subjects showed an increase of the force produced by their muscle under long stimulation, at the beginning of the fatiguing process. The initial value of the force decreased by 50% for 60% of the group at the end of the experiment, whereas 20% of the participants remained between 70% and 100% of their initial value. Under short stimulation, after the fatigue processes, the decrease is strengthened. In Table 2-4 and Figure 2-8, for 60% of the individuals, the peak force elicited from the short pulse trains declined by more than 50% after only 5 trials. While 20% of the subjects exhibited an increase in the peak force from the pretrial values, a decline of more than 60% of the peak force was measured following the final fatigue trial for 90% of subjects.

The instant of maximal force and the final value were used to measure the rate of the force decay under constant stimulation. The force decay rate is measured as the ratio of the difference between the highest normalized value of the force during each stimulation and the final normalized value of the force during the same trial, and the time difference between the moment when the force is the highest and the end of the trial $r_{force\,decay} = \frac{f_{max} - f_{final}}{t_{final} - t_{f_{max}}}$. The measurements are reported in Table 2-5. The force decay is the highest at the beginning, and then decreases, as the force peak decreases. However the variations are too disordered to develop a model.

2.3.3 Gender Comparison

The set of volunteers was equally distributed between men and women. Table 2-7 segregates their respective mean, median, minimal and maximal values of the EMD, to compare the performance of each test group. As suggested by previous research [12, 13], there may be a difference in terms of EMD between men and women. The median, minimal and maximal EMD values for females are 36.9%, 25.2% and 63.2% lower than males, respectively. To determine if the two groups were statistically different, a Student t-test was performed with a significance level of 0.05. The two-sample assuming unequal variances test was realized with Excel for the maximal, minimal, mean, and median values of the EMD. The t-test was unable to reject the null hypothesis. Consequently, maximal, minimal, median or mean EMD for men subjects was not found to be statistically significantly different from the EMD of women subjects. This conclusion supports the results of [10] and [27].

2.3.4 Discussion

Most individuals described the fatigue sensation as a quick and strong increase that became constant. Our findings suggest that EMD varies significantly with NMES-induced fatigue and is in agreement with previous research studying voluntary [14, 15, 18] and NMES-induced contrctions [10]. There are variations in the experimental data in terms of the maximal normalized EMD and the time to reach the maximal relative

EMD. Fatigue was quantified through the measured force during stimulation. While EMD increased to an average value that was twice its initial value, the corresponding force produced by the muscle during stimulation was observed to decrease to less than half of the initial value, in both short and long pulse trains. Moreover, the protocol used did not allow the observation of any significant differences between men and women.

2.4 Characterization of the EMD in Terms of NMES-Induced Fatigue

EMD is correlated to fatigue due to stimulation. The objective in this section is to build a fatigue versus EMD model for each individual. To represent the fatigue, a significant metric is necessary. Different a priori parameters are utilized in Figures 2-10 to 2-12, to determine the most appropriate metric to be used.

2.4.1 First Model: Exponential

Based on the shape of the distribution of the data plotted in Figure 2-11, the following exponential function was developed to fit an approximate curve:

$$\tau = ae^{bx}$$

where τ is defined as the normalized EMD, x denotes the normalized force output, and a and b are unknown fitting coefficients. The exponential function fits the data with values of R^2 greater than 0.5 for 40% of the experiments, that is, the exponential model fits at least half of the variations of the data about the average for these individuals. When applied to the sum of all data, the R^2 value falls to 0.2510 (Figure 2-13). Even if less precise, the predictions bounds for the fitting include 94.12% of all the data points.

2.4.2 Second Model: Sum of Exponentials

The following sum of exponential functions was also used to fit the data: (Figure (2-14))

$$\tau = a_1e^{b_1x} + a_2e^{b_2x} \tag{2–1}$$

where τ is defined as the normalized EMD, x denotes the normalized force output, and $a_{1,2}$ and $b_{1,2}$ are unknown fitting coefficients. With R2 values greater than 0.5 for 90% of the subjects, the exponential model explains more than half of the variation for these individuals. The model was also applied to the combined data set of all subjects resulting in more disparate behaviors among individuals. However, the R^2 value for individuals and for the global fitting were higher (Table 2-9), , reaching an R^2 value of 0.364.. The prediction bounds include 94.59% of the total number of data points.

2.4.3 Conclusion

Our findings suggest that EMD varies significantly with NMES-induced fatigue and is in agreement with previous research with voluntary [14, 15, 18] and NMES-induced contractions [10]. The force production during isometric contractions was an effective metric to track fatigue during stimulation. Thus it was utilized to derive a model for EMD during fatigue. Individual R^2 for the second model were higher than those in the first model. The R^2 corresponding to a global fitting of all the subjects was lower than any individual R^2 but was still higher than in the case of the simple exponential. More than 36% of the variation for all subjects was explained, therefore this is a reasonable model for the evolution of EMD during NMES with respect to fatigue . The relationship between peak force and EMD may be better fitted by a non-exponential model, for small subsets of subjects. Additionally, the reasons for this potential variance among a population of human subjects are not clear at this time.

The model was defined in terms of discrete measures of the force production, for a given voltage value. Because a value of the EMD is needed continuously over the stimulation, (2–1) can be expressed as:

$$\tau = a_1 e^{b_1 f_N / v_N} + a_2 e^{b_2 f_N / v_N} \tag{2–2}$$

where $f_N \in \mathbb{R}^+$ denotes the normalized force output, expressed as the ratio of the actual force over the initial force value f/f_0. $v_N \in \mathbb{R}^+$ is the normalized voltage value used

to measure EMD, and thus can be written as v/v_0, where v is the positive and nonzero actual voltage and v_0 is the positive constant voltage used to determine the initial EMD. Based on these definitions, a measure of the EMD can be expressed continuously while the voltage is varying, with the measure of the corresponding force output. As a result, the actual model of the fatigue-varying EMD for each individual can be obtained with the initial value of the EMD denoted as τ_0 and measured during pre-trial tests:

$$\tau = \tau_0 \left(a_1 e^{b_1 p} + a_2 e^{b_2 p} \right) \tag{2–3}$$

where $\tau \in \mathbb{R}^+$ denotes the current EMD, and τ_0 the initial EMD. The ratio $\frac{f/f_0}{v/v_0}$ is denoted by $p \in \mathbb{R}^+$, where $v_0 \in \mathbb{R}^+$, and $f_0 \in \mathbb{R}^+$ denote respectively the initial voltage input and force output, from a resting situation. Thus $v \in \mathbb{R}^+$ and $f \in \mathbb{R}^+$ correspond to the voltage of the stimulation, and corresponding force produced by the muscle. Finally, a_1, a_2, b_1, and b_2 are fitting coefficients, with $a_1,\, a_2 > 0$ and $b_1,\, b_2 < 0$. Based on the expression in (2–3), the EMD is bounded

$$0 < \tau \leq \tau_0 \left(a_1 e^{b_1 p_{min}} + a_2 e^{b_2 p_{min}} \right) = \varphi_1 \tag{2–4}$$

where $p_{min} \in \mathbb{R}$ is the minimum value achieved by p and $\varphi_1 \in \mathbb{R}^+$ is constant. Provided that $f,\, \dot{f}$ and $v,\, \dot{v}$ are bounded, the rate of change of the EMD can also be bounded

$$|\dot{\tau}| \leq \varphi_2 \tag{2–5}$$

where $\varphi_2 \in \mathbb{R}^+$ is constant.

As EMD may affect FES task performance, the model is developed as a potential aid for designing NMES methods that account for EMD [26].

A) Leg extension machine

B) Force transducer

Figure 2-1. A) Testbed used for the experiment: a leg extension machine, legs are decoupled, and rigid boots are set up to maintain the subject's leg. Adjustments are possible: moving the back of seat forward and backward, as well as moving the boot up and down, depending on the subject's height. B) A force transducer is fixed to the leg extension machine, to measure the force produced by the leg whether the muscle is under stimulation or not. Photos courtesy of Fanny Bouillon.

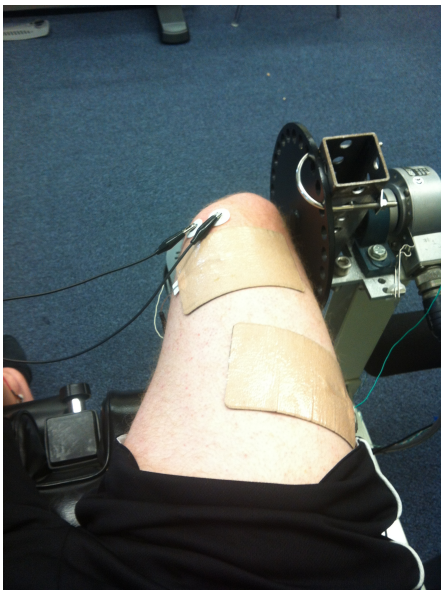

Figure 2-2. Position of the electrode pads for stimulation.Photos courtesy of Kevin Wilt.

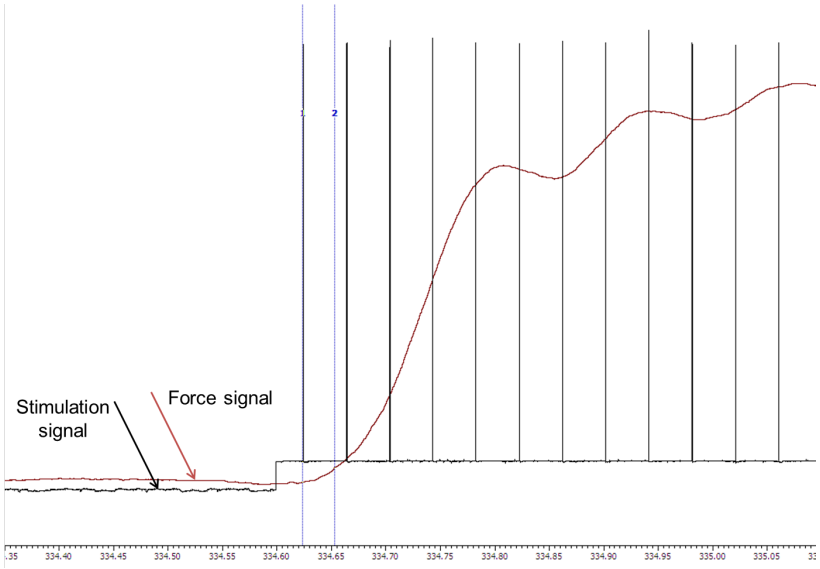

Figure 2-3. Definition of the measurement of the electromechanical delay: time lag between the onset of stimulation (cursor 1) and the first movement of the limb (cursor 2). The cursor 2 is set so that the force value corresponds to 0.2% of the maximal voluntary contraction of the subject.

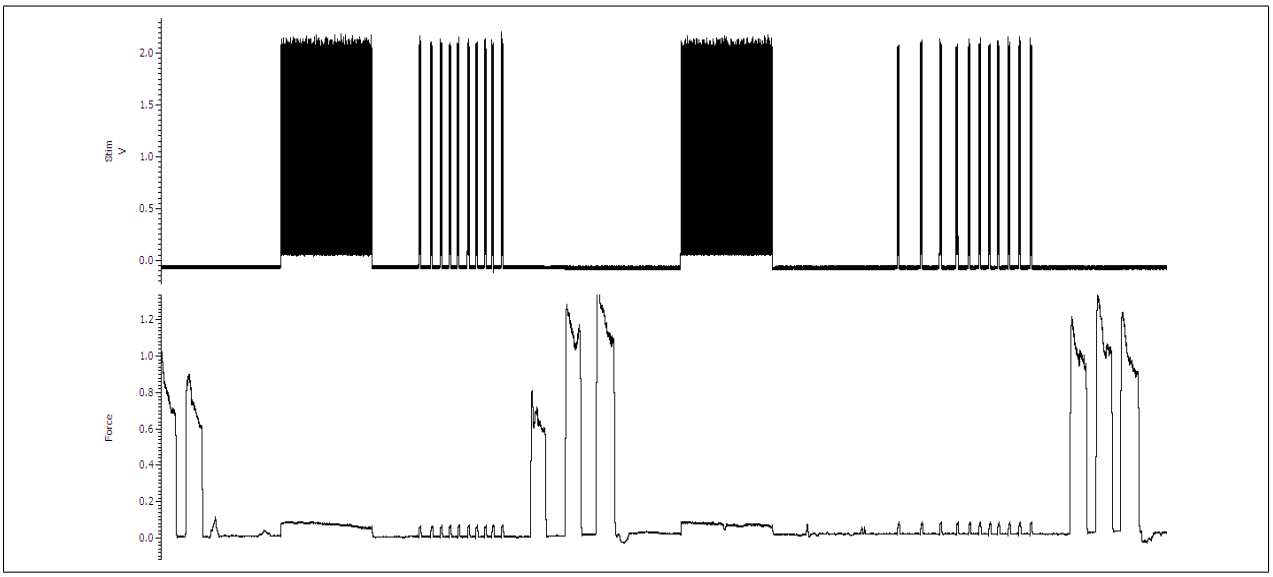

Figure 2-4. Extract of the records of an experiment. Two cycles are shown: the top graph is the non amplified signal of the stimulation, measured in volts. The bottom graph is the signal from the force transducer measuring the force output, normalized with the initial value of the MVC. First, a long train of pulses is sent to stimulate the muscle. Then short pulse trains are applied to measure the EMD. Finally the subject performs voluntary contractions without stimulation.

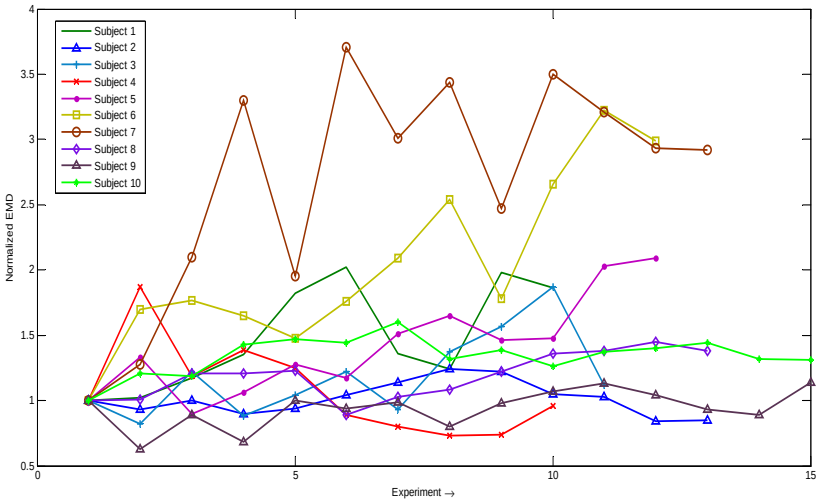

A) Individual curves of evolution of the delay for each individual.

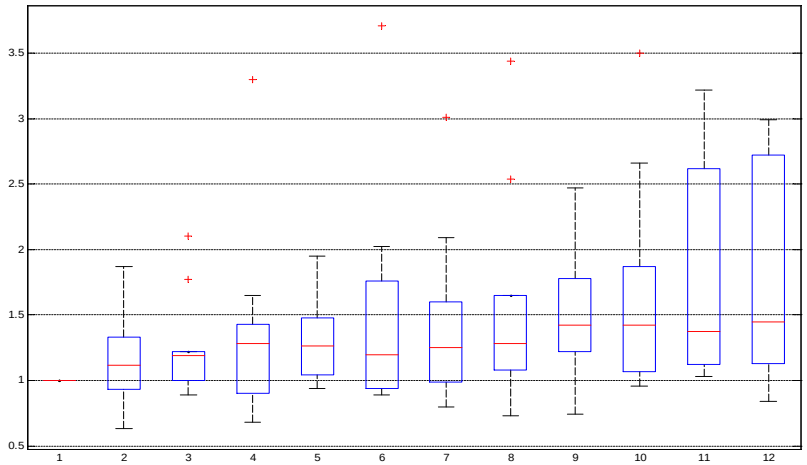

B) Evolution of the distribution of the values of the EMD among the ten subjects.

Figure 2-5. Representation of the EMD throughout the experiment for the ten subjects. A) Individual curves of evolution of the delay for each individual. B) Evolution of the distribution of the values of the EMD among the ten subjects.

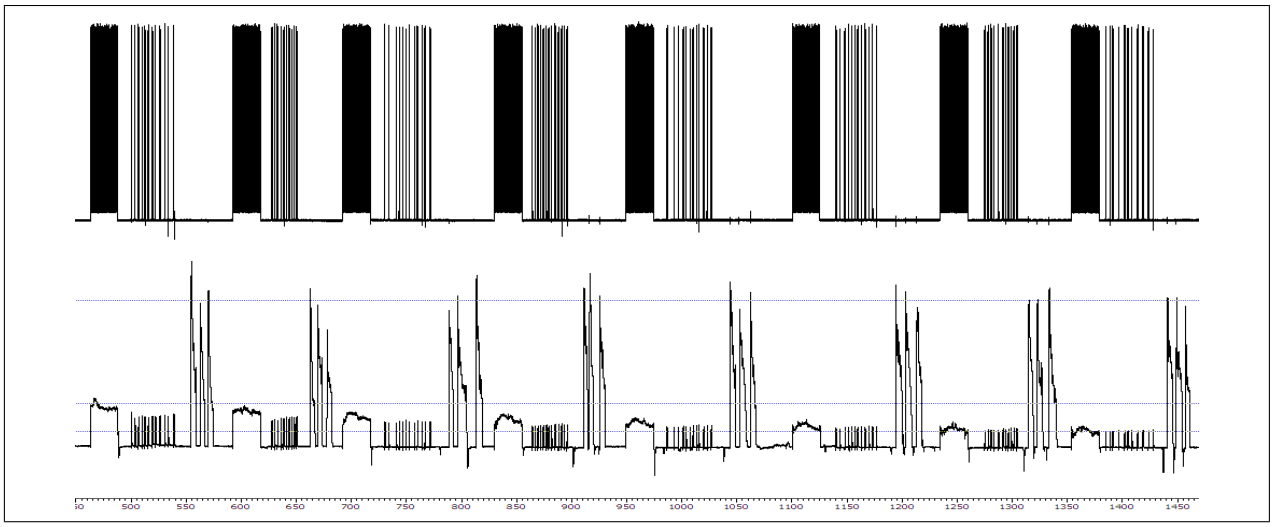

A) First fifty seconds of an experiment.

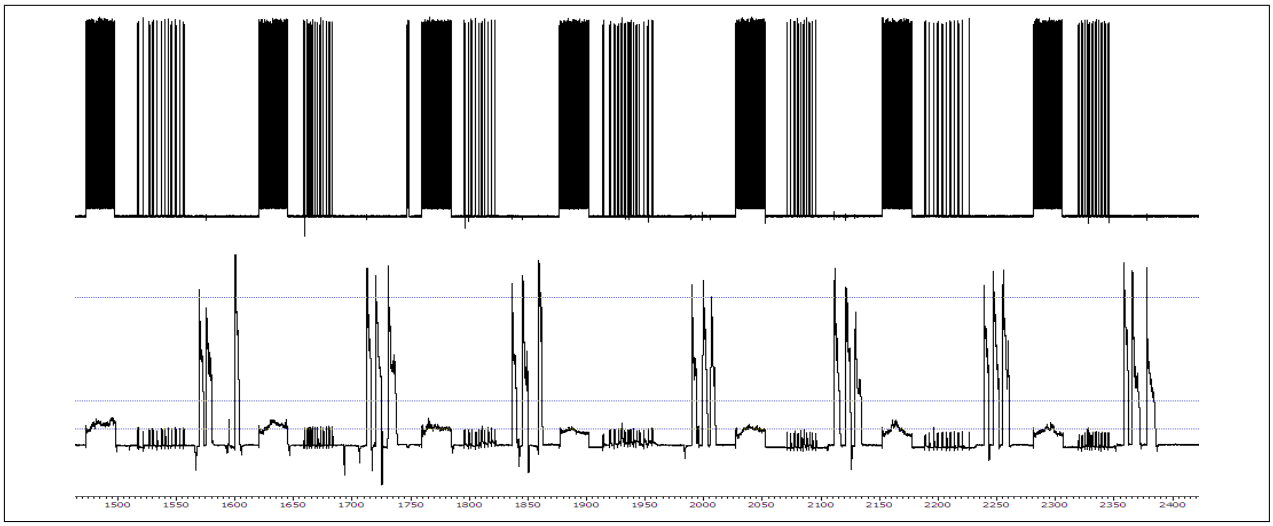

B) Next fifty seconds of the same experiment.

Figure 2-6. Extract of a 100-second experiment, showing the evolution of the normalized force production measurements, while the subject is being stimulated and performs voluntary exercises. A) Zero to 50s. B) Fifty to 100s. The top plots in A) and B) correspond to the stimulation voltage, received by the subjects. The bottom plots in A) and B) represent the force measurements. The horizontal lines are on the same levels on A) and B), corresponding to the average level of the initial forces for both stimulation and voluntary contractions, and the final value reached during stimulation.

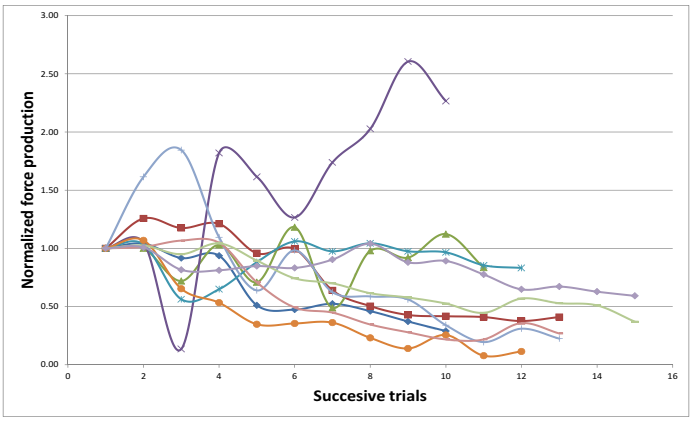

Figure 2-7. Evolution of the highest normalized values of the force produced under long stimulation for the ten experiments.

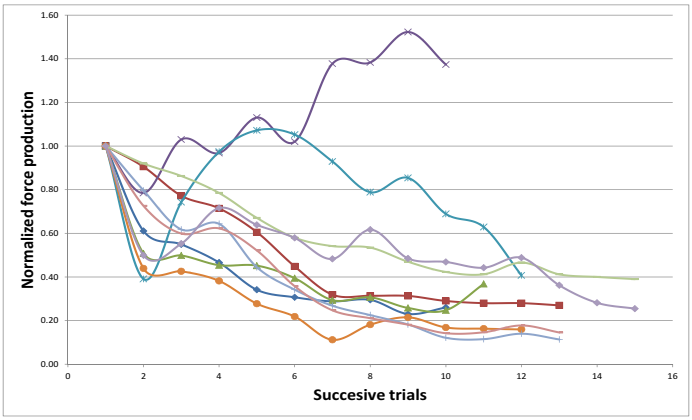

Figure 2-8. Evolution of the normalized values of the force produced under brief stimulation for the ten experiments.

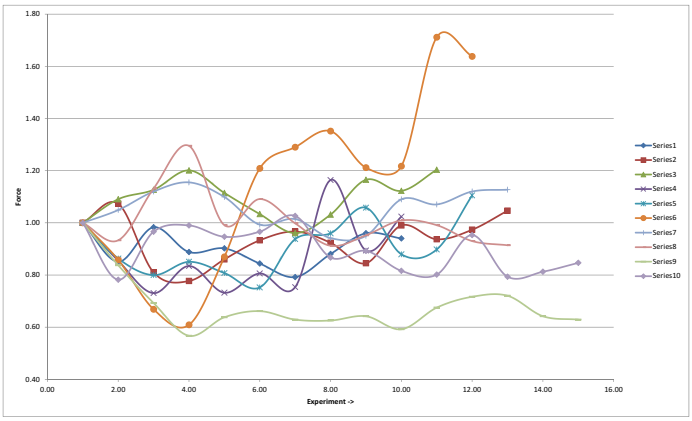

Figure 2-9. Evolution of the maximal voluntary contraction the 10 subjects can perform respectively.

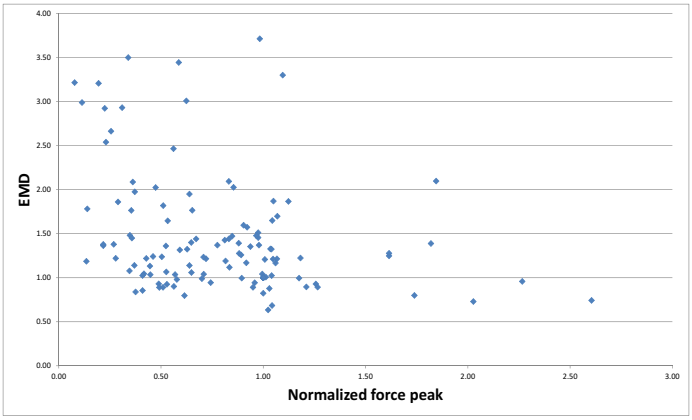

Figure 2-10. EMD versus force peak during long stimulation for the 10 subjects. EMD and force measurements are normalized with their respective values recorded during pretrial test, when the muscle was in a resting position.

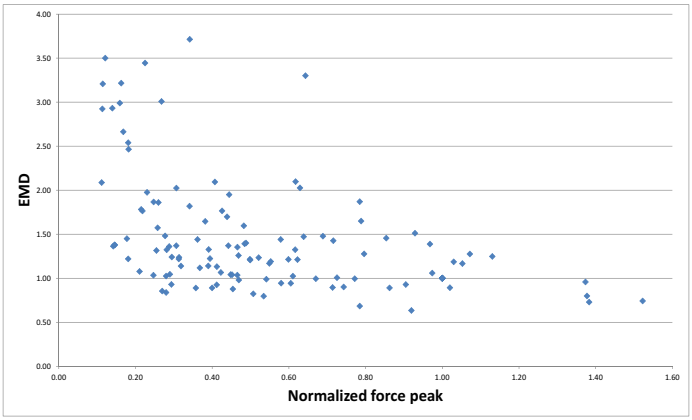

Figure 2-11. EMD versus force output during short pulse trains for the 10 subjects.

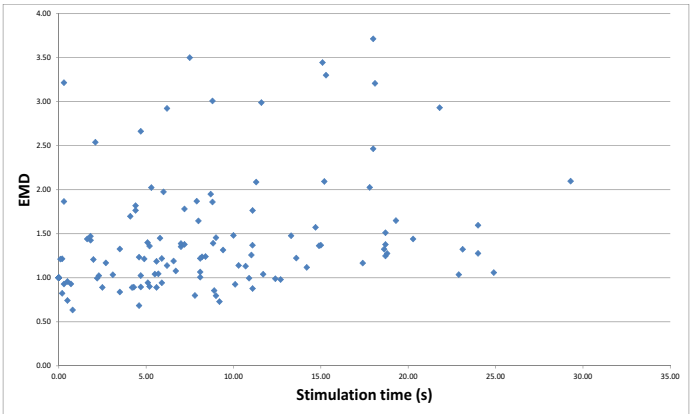

Figure 2-12. EMD versus instant of peak for the 10 subjects. The instant of peak corresponds to the time it took for the force to reach its highest value during a long pulse train.

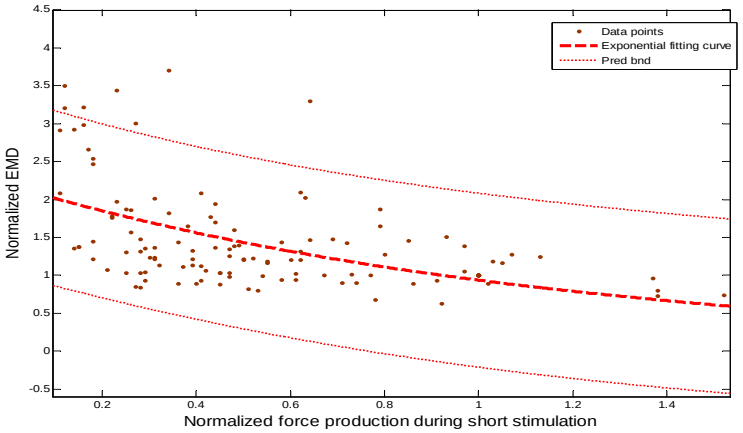

Figure 2-13. Representation of the EMD in terms of the force output produced by the leg. Each point represents the values recorded for all the experiments. The whole set of points can be approximated by an exponential function, represented by the dashed line.

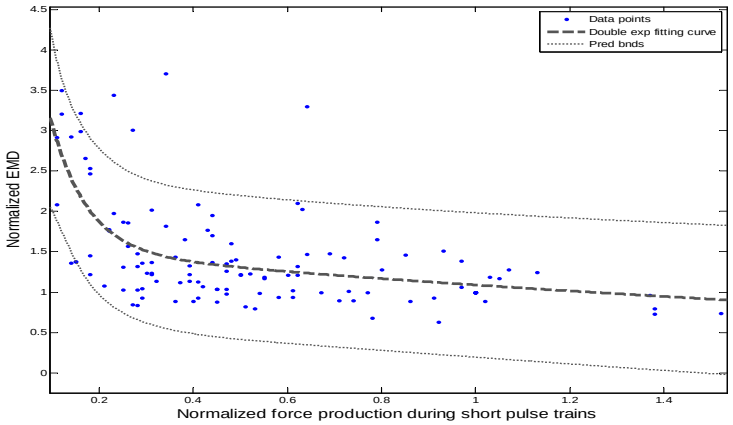

Figure 2-14. Global fitting curve, and respective prediction bounds, of the EMD in terms of the force during short stimulation. The main dashed line represents the double exponential approximation (R^2=0.3637).

Table 2-1. Evolution of the EMD raw values throughout the fatiguing experiment of each of the ten healthy subjects, expressed in seconds. The set number corresponds to the number of long stimulation the subject received, the corresponding EMD is measured immediately following stimulation. The number of fatigue sets depended on the comfort of each subject.

Subject >	1	2	3	4	5	6	7	8	9	10
initial value	0.038	0.052	0.082	0.105	0.048	0.038	0.017	0.040	0.034	0.014
set 1	0.039	0.048	0.068	0.206	0.064	0.065	0.022	0.040	0.022	0.017
set 2	0.044	0.051	0.100	0.124	0.043	0.067	0.036	0.048	0.030	0.017
set 3	0.051	0.046	0.072	0.155	0.051	0.063	0.057	0.048	0.023	0.020
set 4	0.069	0.049	0.086	0.131	0.061	0.056	0.034	0.049	0.034	0.021
set 5	0.077	0.054	0.101	0.093	0.056	0.067	0.064	0.035	0.032	0.020
set 6	0.051	0.059	0.077	0.084	0.073	0.079	0.052	0.041	0.034	0.022
set 7	0.047	0.064	0.113	0.076	0.080	0.097	0.059	0.043	0.027	0.019
set 8	0.075	0.063	0.130	0.078	0.070	0.068	0.042	0.048	0.034	0.020
set 9	0.070	0.054	0.154	0.100	0.071	0.101	0.060	0.054	0.036	0.018
set 10		0.053	0.092		0.100	0.122	0.055	0.055	0.039	0.019
set 11		0.043			0.101	0.114	0.050	0.057	0.035	0.020
set 12		0.044			0.078		0.050	0.055	0.032	0.020
set 13									0.031	0.019
set 14									0.039	0.018
maximal delay	0.077	0.064	0.154	0.206	0.101	0.122	0.064	0.057	0.039	0.022
number of sets to reach maximal delay	5	7	9	1	11	10	5	11	14	6

Table 2-2. Evolution of the EMD throughout the fatiguing experiment of each of the ten healthy subjects. The initial value is set to 1 to normalized each experiment, as absolute values were not to be compared from one subject to another. The set number corresponds to the number of long stimulation the subject received, the corresponding EMD is measured right after it. The number of fatigue sets depended on the pain and comfort situation of each subject.

Subject>	1	2	3	4	5	6	7	8	9	10	Mean	Standard deviation
set 1	1.02	0.93	0.82	1.87	1.33	1.70	1.28	1.01	0.63	1.21	1.18	0.38
set 2	1.17	1.00	1.22	1.19	0.90	1.77	2.10	1.21	0.89	1.19	1.26	0.38
set 3	1.35	0.90	0.88	1.39	1.06	1.65	3.30	1.21	0.68	1.43	1.39	0.74
set 4	1.82	0.94	1.04	1.25	1.28	1.48	1.95	1.23	0.99	1.47	1.35	0.34
set 5	2.02	1.04	1.22	0.89	1.17	1.76	3.71	0.89	0.94	1.44	1.51	0.86
set 6	1.36	1.14	0.93	0.80	1.51	2.09	3.01	1.03	0.99	1.60	1.45	0.67
set 7	1.24	1.24	1.37	0.73	1.65	2.54	3.44	1.08	0.80	1.32	1.54	0.84
set 8	1.98	1.22	1.57	0.74	1.46	1.78	2.47	1.22	0.98	1.39	1.48	0.50
set 9	1.86	1.05	1.87	0.96	1.48	2.66	3.50	1.36	1.07	1.26	1.71	0.81
set 10		1.03	1.12		2.03	3.22	3.21	1.38	1.13	1.37	1.81	0.92
set 11		0.84			2.09	2.99	2.93	1.45	1.04	1.40	1.82	0.87
set 12		0.85					2.92	1.38	0.93	1.44	1.50	0.83
set 13									0.89	1.32	1.11	0.30
set 14									1.14	1.31	1.23	0.12
maximal delay	2.02	1.24	1.87	1.87	2.09	3.22	3.71	1.45	1.14	1.60	2.03	0.82
number of sets to reach maximal delay	5	7	9	1	11	10	5	11	14	6	7.30	4.21

Table 2-3. Measurements of the force produced by the leg: maximum reached during stimulation. Each subject's raw data is normalized in terms of their respective initial value (set to 1).

Subject >	1	2	3	4	5	6	7	8	9	10	Mean	Standard deviation
1	1.04	1.26	1.00	1.05	1.04	1.07	1.62	1.01	1.02	1.01	1.11	0.19
2	0.92	1.18	0.72	0.14	0.56	0.65	1.85	1.07	0.95	0.82	0.89	0.45
3	0.94	1.21	1.03	1.82	0.65	0.53	1.10	1.05	1.04	0.81	1.02	0.35
4	0.51	0.96	0.71	1.62	0.88	0.35	0.64	0.71	0.90	0.85	0.81	0.34
5	0.47	1.00	1.18	1.27	1.06	0.36	0.98	0.49	0.74	0.83	0.84	0.32
6	0.52	0.64	0.49	1.74	0.98	0.36	0.62	0.45	0.70	0.90	0.74	0.40
7	0.46	0.50	0.98	2.03	1.04	0.23	0.59	0.35	0.62	1.04	0.78	0.52
8	0.37	0.43	0.92	2.61	0.98	0.14	0.56	0.28	0.58	0.88	0.78	0.70
9	0.29	0.42	1.12	2.27	0.97	0.26	0.34	0.22	0.53	0.89	0.73	0.63
10		0.41	0.84		0.86	0.08	0.20	0.22	0.45	0.78	0.48	0.31
11		0.38			0.83	0.11	0.31	0.36	0.57	0.65	0.46	0.24
12		0.41					0.23	0.27	0.53	0.67	0.42	0.18
13									0.51	0.63	0.57	0.08
14									0.37	0.59	0.48	0.16

Table 2-4. Measurements of the force output under short pulses (half a second) right after a fatiguing stimulation. Each subject's raw data is normalized in terms of their respective initial value (set to 1).

Subject >	1	2	3	4	5	6	7	8	9	10	Mean	Standard deviation
1	0.61	0.91	0.51	0.79	0.39	0.44	0.80	0.73	0.92	0.50	0.66	0.20
2	0.55	0.77	0.50	1.03	0.74	0.43	0.62	0.60	0.86	0.55	0.67	0.18
3	0.47	0.71	0.45	0.97	0.97	0.38	0.64	0.62	0.78	0.72	0.67	0.20
4	0.34	0.61	0.45	1.13	1.07	0.28	0.44	0.52	0.67	0.64	0.62	0.28
5	0.31	0.45	0.39	1.02	1.05	0.22	0.34	0.36	0.58	0.58	0.53	0.29
6	0.29	0.32	0.29	1.38	0.93	0.11	0.27	0.25	0.54	0.48	0.49	0.39
7	0.30	0.31	0.31	1.38	0.79	0.18	0.23	0.21	0.53	0.62	0.49	0.37
8	0.23	0.31	0.26	1.52	0.85	0.22	0.18	0.18	0.47	0.48	0.47	0.42
9	0.26	0.29	0.25	1.37	0.69	0.17	0.12	0.14	0.42	0.47	0.42	0.38
10		0.28	0.37		0.63	0.16	0.12	0.15	0.41	0.44	0.32	0.18
11		0.28			0.41	0.16	0.14	0.18	0.47	0.49	0.30	0.15
12		0.27					0.11	0.15	0.41	0.36	0.26	0.13
13									0.40	0.28	0.34	0.08
14									0.39	0.25	0.32	0.10

Table 2-5. Values of the force decay rate under stimulation, expressed in s^{-1}: measured as the speed at which the normalized force is decreasing after having reached its maximum of the stimulation.

Subject >	1	2	3	4	5	6	7	8	9	10	Mean	Standard deviation
1	-0.42	-0.51	-0.42	-0.40	-0.12	-1.00	-0.62	-1.00	-0.23	-0.33	-0.51	0.30
2	-1.00	-0.78	-0.68	0.17	-0.95	-0.52	0.34	-0.77	-0.32	-0.48	-0.50	0.45
3	-0.91	-1.00	-1.00	-0.72	0.00	-0.31	-0.15	-0.49	-0.29	-0.04	-0.49	0.39
4	-0.61	-0.87	-0.44	-0.96	-0.46	-0.91	-0.23	-0.48	-0.38	-0.40	-0.57	0.25
5	-0.58	-0.84	-0.59	-0.24	-1.00	-0.55	-1.00	-0.20	-0.27	-0.40	-0.57	0.30
6	-0.69	-0.48	-0.04	-0.79	-0.81	-0.61	-0.34	-0.19	-0.56	-0.70	-0.52	0.26
7	-0.64	-0.37	0.00	-0.87	-0.28	-0.34	-0.60	-0.43	-0.22	-0.33	-0.41	0.24
8	-0.62	-0.23	-0.17	-1.00	-0.12	-0.18	-0.67	-0.33	-0.39	-1.00	-0.47	0.33
9	-0.42	-0.21	-0.47	-0.72	-0.26	-0.85	-0.16	-0.24	-0.34	-0.95	-0.46	0.28
10		-0.22	-0.40		-0.44	-0.11	-0.09	-0.32	-0.29	-0.59	-0.31	0.17
11		-0.18			-0.47	-0.20	-0.40	-0.38	-1.00	-0.13	-0.39	0.30
12		-0.32					-0.06	-0.35	-0.34	-0.77	-0.37	0.25
13									-0.37	-0.28	-0.33	0.06
14									-0.30	-0.21	-0.26	0.06

Table 2-6. Voluntary contractions measurements. The force produced by each of the subjects when they perform maximal voluntary contractions is reported in this table. Each value is normalized with the initial performance of the corresponding subject.

Subject >	1	2	3	4	5	6	7	8	9	10	Mean	Standard deviation
1	0.85	1.07	1.09	0.86	0.86	0.86	1.05	0.93	0.84	0.78	0.92	0.11
2	0.98	0.81	1.13	0.73	0.80	0.67	1.12	1.13	0.69	0.97	0.90	0.19
3	0.89	0.78	1.20	0.83	0.85	0.61	1.16	1.30	0.57	0.99	0.92	0.24
4	0.90	0.86	1.11	0.73	0.81	0.87	1.10	0.99	0.64	0.95	0.90	0.15
5	0.84	0.93	1.03	0.81	0.75	1.21	0.99	1.09	0.66	0.97	0.93	0.17
6	0.79	0.97	0.96	0.75	0.94	1.29	1.01	1.00	0.63	1.03	0.94	0.18
7	0.88	0.92	1.03	1.16	0.96	1.35	0.94	0.91	0.63	0.87	0.97	0.19
8	0.96	0.85	1.17	0.89	1.06	1.21	0.95	0.95	0.64	0.89	0.96	0.16
9	0.94	0.99	1.12	1.02	0.88	1.22	1.09	1.01	0.59	0.82	0.97	0.18
10		0.94	1.20		0.90	1.71	1.07	0.99	0.68	0.80	1.04	0.32
11		0.97			1.11	1.64	1.12	0.93	0.72	0.95	1.06	0.29
12		1.05					1.13	0.91	0.72	0.79	0.92	0.17
13									0.64	0.81	0.73	0.12
14									0.63	0.85	0.74	0.16

Table 2-7. Segregation of the mean, median, maximal and minimal values of the EMD, expressed in seconds, of men and women. The values reported here were used to test the difference between the two groups through a Student t-test., and the result of the test for each parameter is reported in the last row of the table.

	Mean EMD	Median EMD	Maximum EMD	Minimum EMD
Men	0.056	0.051	0.077	0.038
	0.052	0.052	0.064	0.043
	0.078	0.068	0.122	0.038
	0.115	0.103	0.206	0.076
	0.069	0.070	0.101	0.043
Women	0.046	0.050	0.064	0.017
	0.047	0.048	0.057	0.035
	0.032	0.034	0.039	0.022
	0.019	0.019	0.022	0.014
	0.098	0.092	0.154	0.068
P	0.089	0.117	0.103	0.111

Table 2-8. Coefficients of determination following an exponential curve fit of the form $\tau = ae^{bx}$

Subject #	R^2	Subject #	R^2
1	0.5718	6	0.5508
2	0.0852	7	0.5226
3	0.2802	8	0.2834
4	0.7243	9	0.3067
5	0.3091	10	0.1437
ALL		0.2510	

Table 2-9. The coefficient of determination following a curve fit of the form $\tau = a_1e^{b_1x} + a_2e^{b_2x}$.

Subject #	R^2	Subject #	R^2
1	0.6326	6	0.5816
2	0.6015	7	0.6217
3	0.6669	8	0.5358
4	0.8125	9	0.5226
5	0.5108	10	0.4628
ALL		0.3637	

CHAPTER 3
TIME-VARYING ELECTROMECHANICAL DELAY COMPENSATION IN NEUROMUSCULAR ELECTRICAL STIMULATION

The motivation to improve the NMES rehabilitation comfort and performances leads to the objective of adapting the stimulation intensity applied to the current state of the muscle. This chapter adapts a controller, designed to compensate for time-varying input delay in nonlinear systems, to FES.

3.1 Muscle Stimulation Model

The musculoskeletal dynamics with one degree of freedom corresponding to the rotation about the knee joint, is defined as [28]

$$M_e + M_g + M_v + M_I + d = T\left(t - \tau\left(t\right)\right) \tag{3–1}$$

where $M_I\left(\ddot{q}\right) \in \mathbb{R}$ corresponds to the inertia of the shank-foot system, $M_e\left(q\right) \in \mathbb{R}$ denotes the elastic effects due to joint stiffness, $M_g\left(q\right) \in \mathbb{R}$ denotes the gravitational component, and $M_v\left(\dot{q}\right) \in \mathbb{R}$ the viscous effect due to damping in the musculotendon complex, $d\left(t\right) \in \mathbb{R}$ represents unknown bounded disturbances, and $T\left(t - \tau\left(t\right)\right) \in \mathbb{R}$ corresponds to the torque produced at the knee joint by the electrical stimulation. The generalized states are defined as $q\left(t\right), \dot{q}\left(t\right), \ddot{q}\left(t\right) \in \mathbb{R}^n$ and correspond to the angular position, velocity and acceleration of the lower limb. The inertia component is defined as $M_I\left(\ddot{q}\right) = J\ddot{q}$ where $J \in \mathbb{R}$ denotes the unknown inertia of the shank-foot system. The gravitational effects can be modeled as $M_g\left(q\right) = mgl\sin\left(q\right)$ where m, g, $l \in \mathbb{R}$ respectively are the unknown mass of the system, the unknown distance between the knee joint and the mass center, and the gravitational acceleration. The elastic effects are defined as $M_e\left(q\right) = k_1 e^{-k_2 q}\left(q - k_3\right)$ where k_1, k_2, $k_3 \in \mathbb{R}$ are unknown positive constants. Finally, the viscous effects are defined as $M_v = B_1 \tanh\left(-B_2\dot{q}\right) + B_3\dot{q}$ where B_1, B_2, $B_3 \in \mathbb{R}$ are unknown positive constants.

The knee torque is related to the muscle tendon force $F\left(q, \dot{q}, t\right)$ through $T = \zeta F$ where $\zeta\left(q\right)$ is a positive unknown nonlinear moment arm. The muscle force generated at

the tendon is expressed as $F = \Gamma V$ where $V(t)$ is the voltage applied and $\Gamma(q, \dot{q})$ is an unknown nonlinear function.

Assumption1 The moment arm is assumed to be a non-zero, positive and bounded function whose first and second time derivatives exist. The function Γ is assumed to be non zero, positive and bounded function, whose first and second time derivatives exist and are bounded.

Assumption2 The first and second time derivatives of an auxiliary non-zero, unknown scalar function $\Omega(q, \dot{q})$, defined as $\Omega = \zeta\Gamma$, are assumed to exist and be bounded.

Assumption3 The unknown disturbance $d(t)$ is bounded, as well as its first and second time derivatives.

Equation (3–1) can be rewritten as

$$\ddot{q} = f(q, \dot{q}, t) + d + u(t - \tau(t)) \tag{3–2}$$

where

$$f(q, \dot{q}, t) = \frac{1}{J}\left(-mgl\sin(q) - k_1 e^{-k_2 q}(q - k_3) - B_1 \tanh(-B_2\dot{q}) - B_3\dot{q}\right) \tag{3–3}$$

is a nonlinear unknown $\mathcal{C}^2$ function, uniformly bounded in t, d corresponds to smooth disturbances, u denotes the delayed control input, and τ the positive time-varying input delay.

Assumption4 The nonlinear disturbance term and its first two time derivatives exist and are bounded by known constants.

Assumption5 The desired trajectory $q_d \in \mathbb{R}$ is designed such that $q_d^{(i)}$, $\forall i \in [\![0, 4]\!]$ exist and are bounded by known positive constants, where $q_d^{(i)}$ denotes the i^{th} time derivative of q_d.

Assumption6 The input delay is bounded such that $0 \leq \tau \leq \varphi_1$ and the rate of change of the delay is bounded such that $|\dot{\tau}| \leq \varphi_2 < 1$ where $\varphi_{1,2}$ are known constants, and $\varphi_1 + \varphi_2 < 1$.

3.2 Input Delay Model

The fatigue-varying electromechanical delay model (2–1) that was determined in Chapter 3 was ultimately to be utilized for FES. However, the model was developed under isometric conditions and requires force measurements. Experiments allow the measure of the force, but the resulting output signal has a large signal to noise ratio without the use of a low-pass filter. Thus additional lag would be added to the force signal, interfering with the EMD compensation. Moreover, position tracking involves the movement of the lower limb. A new set up of the leg extension machine has to be done, to give the leg its rotational degree of freedom about the knee. However, the value that will be measured will not correspond to the muscle production force. To retrieve this quantity, and use the model in the previous chapter, additional modeling of the muscle, and sensors would be necessary.

Instead of adding sensors, the input delay will be modeled as a function of time. To do so, electrical pulses are successively applied to the lower limb, and the EMD is measured as the time lag between the onset of stimulation and the onset of the movement of the leg. This latter is defined as 0.02% of the maximal reference angle. Then an expression, involving time, is derived to fit the evolution of the EMD. This expression corresponds to the time-varying input delay model, and is specific to a reference trajectory. The measure of the EMD and its modeling will be detailed in the Experimental Results Section.

3.3 Control Design

3.3.1 Previous Approaches

Linear systems are well controlled in various ways in the literature [29–34], including constant input delay issues for linear systems [35–37]. These results were also extended later for time-varying input delays [38–44]. Nonlinear systems have also been studied, whether they involve constant [45–52] or time-varying [45, 53–62] state delays, but input delays in uncertain systems have received less consideration. However

backstepping and robust techniques were used [61, 63–65], as well as predictor-based techniques [37, 64, 65], but required no disturbances. For this study, the controller in [61] was utilized and adapted to neuromuscular electrical stimulation. To compensate for the input delay, a predictor-like error signal based on previous control values is used to yield a delay-free open-loop system, allowing control design flexibility. A Lyapunov stability analysis then demonstrates the achievement of semi-global asymptotic tracking in the presence of model uncertainty, smooth disturbances and time-varying input delay.

3.3.2 Robust Integral of the Sign of the Error control technique (RISE)

3.3.2.1 Control objective

To quantify the control objective, the tracking error $e_1 \in \mathbb{R}$ is defined as

$$e_1 = q_d - q \tag{3–4}$$

Moreover, two auxiliary tracking errors $e_2 \in \mathbb{R}$ and $r \in \mathbb{R}$ are defined as

$$e_2 = \dot{e_1} + \alpha_1 e_1 \tag{3–5}$$

$$r = \dot{e_2} + \alpha_2 e_2 + e_u \tag{3–6}$$

where $\alpha_1,\ \alpha_2$ are positive real constant control gains, and $e_u \in \mathbb{R}$ is the difference between the delayed control input and the actual control input defined as

$$e_u = u\left(t - \tau\left(t\right)\right) - u\left(t\right) \tag{3–7}$$

Furthermore, an auxiliary filter $e_{uf} \in \mathbb{R}$ is defined as the solution to the differential equation

$$\dot{e_{uf}} = -\alpha_2 e_{uf} + e_u \tag{3–8}$$

Substituting (3–8) into (3–6) allows (3–6) to be expressed as

$$r = \dot{\eta} + \alpha_2 \eta \tag{3–9}$$

where $\eta \in \mathbb{R}$ is defined as

$$\eta = e_2 + e_{uf} \tag{3–10}$$

Then substituting for $\dot{\eta}$ into r gives

$$r = \ddot{q}_d - f\left(q, \dot{q}, t\right) - d - u\left(t - \tau\right) + \alpha_1 \dot{e}_1 + \dot{e}_{uf} + \alpha_2 \eta. \tag{3–11}$$

To obtain the open-loop tracking error, (3–8), (3–7) and (3–10) are substituted in (3–11), and then some algebraic manipulation $f\left(q_d, \dot{q}_d, t\right)$, leads to

$$r = S_1 + S_2 - u \tag{3–12}$$

where $S_1,\ S_2 \in \mathbb{R}$ are defined as

$$S_1 = f\left(q_d, \dot{q}_d, t\right) - f\left(q, \dot{q}, t\right) + \alpha_1 \dot{e}_1 + \alpha_2 e_2 \tag{3–13}$$

$$S_2 = \ddot{q}_d - f\left(q_d, \dot{q}_d, t\right) - d. \tag{3–14}$$

The use of (3–7) eliminates the delayed terms.

Based on the open-loop dynamics in (3–12), the controller is designed as

$$u = \left(k_s + 1\right)\left(e_2 - e_2\left(t_0\right)\right) + \nu \tag{3–15}$$

where v is the Filippov solution to

$$\dot{\nu} = \left(k_s + 1\right)\left(\alpha_2 e_2 + e_u\right) + \beta sgn\left(\eta\right) \tag{3–16}$$

and k_s and β are positive constant control gains. The existence of Filippov solutions can be established for $\dot{v} \in K\left[h_1\right]\left(e_2, e_u, \eta\right)$, where $h_1 \in \mathbb{R}$ is defined as the right-hand side of (3–16), and $K\left[h_1\right] \triangleq \bigcap_{\delta>0} \bigcap_{\mu(S_m)=0} \overline{co} h_1\left(e_2, e_u, B\left(\eta, \delta\right) - S_m\right)$, where $\delta \in \mathbb{R}$, $\bigcap_{\mu(S_m)=0}$ denotes

the intersection over sets S_m of Lebesgue measure zero, $\overline{co}$ denotes convex closure, and $B(\eta, \delta) = \{\varsigma \in \mathbb{R}^n | \ \|\eta - \varsigma\| < \delta\}$ [66, 67].

Thus the closed-loop error system can be written

$$\dot{r} = \tilde{N} + N_d - e_2 - (k_s + 1) r - \beta sgn(\eta) \tag{3–17}$$

with

$$\tilde{N} = \dot{S}_1 + e_2 \text{ and } N_d = \dot{S}_2. \tag{3–18}$$

The following inequalities can be developed from the expression in (3–18) and the Mean Value Theorem:

$$\|\tilde{N}\| \leq \rho(\|z\|) \|z\| \tag{3–19}$$

where

$$z \triangleq \left[e_1^T, e_2^T, r^T, e_u^T\right]^T \tag{3–20}$$

and ρ is a positive, non decreasing and invertible function. The expression in (3–18) can also be upper-bounded as

$$\|N_d\| \leq \zeta_{N_{d1}} \ \ \|\dot{N}_d\| \leq \zeta_{N_{d2}} \tag{3–21}$$

where $\zeta_{N_{d1}}$, $\zeta_{N_{d2}}$ are known positive constants, and let $\acute{z} \in \mathbb{R}^3$ be defined as

$$\acute{z} \triangleq \left[e_1^T, \ e_2^T, \ r^T\right]^T. \tag{3–22}$$

To facilitate the subsequent analysis, an auxiliary constant σ is defined as

$$\sigma \triangleq \min\left\{\alpha_1 - \frac{1}{2}, \alpha_2 - 1, \frac{4k_s}{3} - \omega\varphi_1 (k_s + 1)^2, \frac{\omega(1 - \varphi_1 - \varphi_2)}{\varphi_1}\right\}, \tag{3–23}$$

where ω is a known adjustable positive constant.

3.3.2.2 Stability analysis

Theorem 1. *The controller in (3–15) and (3–16) ensures uniformly ultimately bounded stability in the sense that*

$$\|e_1(t)\| \leq \epsilon_0 \exp(-\epsilon_1 t) + \epsilon_2, \tag{3–24}$$

where $\epsilon_0,\ \epsilon_1,\ \epsilon_2 \in \mathbb{R}$ *are positive constants, and provided the control gains satisfy the following conditions:*

$$\alpha_1 > \frac{1}{2} \tag{3–25}$$

$$\alpha_2 > 1 \tag{3–26}$$

$$\beta > \zeta_{N_{d1}} + \frac{\zeta_{N_{d2}}}{\alpha_2} \tag{3–27}$$

$$4\sigma k_s > 3\rho^2(\|z(t_0)\|) \tag{3–28}$$

$$\omega > \frac{\varphi_1}{2(1-\varphi_1-\varphi_2)} \tag{3–29}$$

$$\frac{k_s}{(k_s+1)^2} > 3\omega\varphi_1. \tag{3–30}$$

PROOF. Let $\mathscr{D} \triangleq \left\{ y \in \mathbb{R}^5 \mid \|\acute{y}\| < \rho^{-1}\left(\sqrt{\frac{4\sigma k_s}{3}}\right) \right\}$, where $\acute{y} \triangleq \left[y^T,\ e_u^T\right]^T \in \mathbb{R}^6$, be an open and connected set containing $y = 0$, where $y \in \mathbb{R}^5$ is defined as

$$y \triangleq \begin{bmatrix} \acute{z}^T & \sqrt{P} & \sqrt{Q} \end{bmatrix}^T. \tag{3–31}$$

In (3–31), the auxiliary function $P \in \mathbb{R}$ is defined as a Filippov solution to the following differential equation

$$\begin{aligned} \dot{P} &= -r^T(N_d - \beta sgn(\eta)), \\ P(t_0) &= \beta \sum_{i=1}^{n} |\eta_i(t_0)| - \eta_i(t_0)^T N_d(t_0) \end{aligned} \tag{3–32}$$

where the subscript $i = 1, 2, ..., n$ denotes the i^{th} element of a vector. Similar to the development in (3–16), existence of solutions P for (3–32) can be established. Provided

the sufficient condition for β in (3–27) is satisfied, $P(t) \geq 0, \ \forall t \in [0, \infty)$ (See the Appendix A for details). Additionally, let $Q \in \mathbb{R}$ denote an LK functional, defined as

$$Q \triangleq \omega \int_{t-\tau(t)}^{t} \left(\int_{s}^{t} \|\dot{u}(\theta)\|^2 d\theta \right) ds \tag{3–33}$$

where ω was introduced in (3–23).

Let $V : \mathscr{D} \to \mathbb{R}$ be a continuously differentiable function defined as

$$V \triangleq \frac{1}{2} e_1^T e_1 + \frac{1}{2} e_2^T e_2 + \frac{1}{2} r^T r + P + Q \tag{3–34}$$

which satisfies the following inequalities:

$$\lambda_1 \|y\|^2 \leq V(y) \leq \lambda_2 \|y\|^2 \tag{3–35}$$

where $\lambda_1, \lambda_2 \in \mathbb{R}^+$ are positive constants. Consider a set

$$B_\sigma \triangleq \left\{ y \in \mathscr{D} \mid \|y\| < \rho^{-1} \left(\sqrt{\frac{4\sigma k_s}{3}} \right) \right\} \subset \mathscr{D} \tag{3–36}$$

and let $S_{\mathscr{D}} \subset B_\sigma$ be defined as

$$\mathcal{S}_{\mathscr{D}} \triangleq \left\{ y \in B_\sigma \mid \|y\| < \sqrt{\frac{\lambda_1}{\lambda_2}} \rho^{-1} \left(\sqrt{\frac{4\sigma k_s}{3}} \right) \right\}. \tag{3–37}$$

Let y be a Filippov solution to the closed-loop system $\dot{y} = h_3(y, t)$ such that $y(t_0) \in S_{\mathscr{D}}$, where $h_3 : \mathbb{R}^6 \times [0, \infty) \to \mathbb{R}^6$ denotes the right-hand side of the closed-loop error system. The time derivative of (3–34) exists almost everywhere (a.e.), i.e., for almost all $t \in [t_0, t_f]$, and $\dot{V}(y(t)) \overset{a.e.}{\in} \dot{\tilde{V}}(y(t))$ where $\dot{\tilde{V}} = \bigcap_{\xi \in \partial V_L(y)} \xi^T K \left[\dot{e}_1^T, \dot{e}_2^T, \dot{r}^T, \frac{P^{-\frac{1}{2}} \dot{P}}{2}, \frac{Q^{-\frac{1}{2}} \dot{Q}}{2} \right]^T$, and ∂V is the generalized gradient of V [68]. Throughout the subsequent discussion, let a.e. refer to almost all $t \in [0, \infty)$. Since V is continuously differentiable,

$$\dot{\tilde{V}} \subset \nabla V^T K \left[\dot{e}_1^T, \dot{e}_2^T, \dot{r}^T, \frac{P^{-\frac{1}{2}} \dot{P}}{2}, \frac{Q^{-\frac{1}{2}} \dot{Q}}{2} \right]^T \tag{3–38}$$

where $\nabla V \triangleq \left[e_1^T, \ e_2^T, \ r^T, \ 2P^{\frac{1}{2}}, \ 2Q^{\frac{1}{2}} \right]^T$. Using the calculus for K from [67], applying the Leibniz Rule to determine the time derivative of (3–33), and substituting (3–4)-(3–6),

(3–17), and (3–32) into (3–38), yields

$$\dot{\tilde{V}} \subset e_1^T\left(e_2-\alpha_1 e_1\right)+e_2^T\left(r-\alpha_2 e_2-e_u\right)+r^T\left(\tilde{N}+N_d-e_2-\left(k_s+1\right) r-\beta K\left[sgn\left(\eta\right)\right]\right)$$
$$-r^T\left(N_d-\beta K\left[sgn\left(\eta\right)\right]\right)+\omega\tau\left(k_s+1\right)^2\left\|r\right\|^2+\omega\tau\beta^2+2\omega\tau\left(k_s+1\right)\beta r^T K\left[sgn\left(\eta\right)\right]$$
$$-\omega\left(1-\dot{\tau}\right)\int_{t-\tau(t)}^{t}\left\|\dot{u}\left(\theta\right)\right\|^2 d\theta \tag{3–39}$$

where $K\left[sgn(e_2)\right]=SGN\left(e_2\right)$ such that $SGN\left(e_{2_i}\right)=1$ if $e_{2_i}>0$, $[-1,1]$ if $e_{2_i}=0$, and -1 if $e_{2_i}<0$ [67]. After canceling common terms, the expression in (3–40) can be upper bounded as

$$\dot{V} \overset{a.e.}{\leq} -\alpha_1\left\|e_1\right\|^2-\alpha_2\left\|e_2\right\|^2-\left(k_s+1\right)\left\|r\right\|^2+\left\|e_1\right\|\left\|e_2\right\|+\left\|e_2\right\|\left\|e_u\right\|$$
$$+\left\|r\right\|\rho\left(\left\|z\right\|\right)\left\|z\right\|+\omega\varphi_1\left(k_s+1\right)^2\left\|r\right\|^2+\omega\varphi_1\beta^2$$
$$+2\omega\varphi_1\left(k_s+1\right)\beta\left\|r\right\|-\omega\left(1-\dot{\tau}\right)\int_{t-\tau(t)}^{t}\left\|\dot{u}\left(\theta\right)\right\|^2 d\theta \tag{3–40}$$

where the set in (3–40) reduces to the scalar inequality in (3–40) since the RHS is continuous a.e., i.e, the RHS is continuous except for the Lebesgue negligible set of times when[1] $r^T\beta K\left[sgn\left(\eta\right)\right]-r^T\beta K\left[sgn\left(\eta\right)\right]\neq\{0\}$. Using (3–6), (3–21), (3–19), and Young's Inequality to show that

$$\left\|e_1^T e_2\right\|\leq\frac{1}{2}\left\|e_1\right\|^2+\frac{1}{2}\left\|e_2\right\|^2 \text{ and } \left\|e_2^T e_u\right\|\leq\frac{1}{2}\left\|e_2\right\|^2+\frac{1}{2}\left\|e_u\right\|^2,$$

[1] The set of times $\Lambda\triangleq\left\{t\in[0,\infty):r\left(t\right)^T\beta K\left[sgn\left(\eta\left(t\right)\right)\right]-r\left(t\right)^T\beta K\left[sgn\left(\eta\left(t\right)\right)\right]\neq\{0\}\right\}\subset[0,\infty)$ is equal to the set of times $\{t:\eta\left(t\right)=0\ \wedge r\left(t\right)\neq 0\}$. From (3–9), this set can also be represented by $\{t:\eta\left(t\right)=0\ \wedge\dot{\eta}\left(t\right)\neq 0\}$. Since $\eta:[0,\infty)\to\mathbb{R}^n$ is continuously differentiable, it can be shown that the set of time instances$\{t:\eta\left(t\right)=0\ \wedge\dot{\eta}\left(t\right)\neq 0\}$ is isolated, and thus, measure zero; hence, Λ is measure zero.

the expression in (3–40) can be upper bounded as

$$\dot{V} \overset{a.e.}{\leq} -\left(\alpha_1 - \frac{1}{2}\right)\|e_1\|^2 - (\alpha_2 - 1)\|e_2\|^2 - \|r\|^2 - \left(\frac{k_s}{3} - \omega\varphi_1 (k_s+1)^2\right)\|r\|^2 + \frac{1}{2}\|e_u\|^2 + \omega\varphi_1\beta^2 - \frac{k_s}{3}\|r\|^2 + 2\omega\varphi_1 (k_s+1)\beta\|r\| - \omega(1-\dot{\tau})\int_{t-\tau(t)}^{t}\|\dot{u}(\theta)\|^2 d\theta - \frac{k_s}{3}\|r\|^2 + \|r\|\rho(\|z\|)\|z\|. \tag{3–41}$$

By completing the squares for $\|r\|$ and by utilizing the facts that $\|e_u\|^2 \leq \tau\int_{t-\tau(t)}^{t}\|\dot{u}(\theta)\|^2 d\theta$, the expression in (3–41) can be upper bounded as

$$\dot{V} \overset{a.e.}{\leq} -\left(\alpha_1 - \frac{1}{2}\right)\|e_1\|^2 - (\alpha_2 - 1)\|e_2\|^2 - \left(1 + \frac{k_s}{3} - \omega\varphi_1 (k_s+1)^2\right)\|r\|^2 + \frac{3\rho^2(\|z\|)\|z\|^2}{4k_s} + \omega\varphi_1\beta^2 + \frac{3(\omega\varphi_1 (k_s+1)\beta)^2}{k_s} - \left(\frac{\omega(1-\dot{\tau}) - \omega\tau - \frac{\tau}{2}}{\tau}\right)\|e_u\|^2. \tag{3–42}$$

If the conditions in (3–25) to (3–30) are satisfied, based on the fact that $\|z\|^2 \geq \|\dot{z}\|^2$, the expression in (3–42) reduces to

$$\dot{V} \overset{a.e.}{\leq} -\left(\sigma - \frac{3\rho^2(\|z\|)}{4k_s}\right)\|z\|^2 + c_2 \leq -c_1\|\dot{z}\|^2 + c_2, \tag{3–43}$$

for all $y \in \mathscr{D}$, for some constants

$$c_1 = \sigma - \frac{3\rho^2(\|z\|)}{4k_s} \in \mathbb{R}^+,\ c_2 = \omega\varphi_1\beta^2 + \frac{3(\omega\varphi_1 (k_s+1)\beta)^2}{k_s} \in \mathbb{R}^+$$

and where σ and $\rho(\|z\|)$ were introduced in (3–28). The inequalities in (3–35) can be used to show that

$$\dot{V} \overset{a.e.}{\leq} -\frac{c_1}{\lambda_1}V + \epsilon \tag{3–44}$$

where $\epsilon \in \mathbb{R}$ is a positive constant. The differential equation in (3–44) can be solved as

$$V(t) \leq V(0)\exp\left(-\frac{c_1}{\lambda_1}t\right) + \frac{c_2}{c_1}\lambda_1\left(1 - \exp\left(-\frac{c_1}{\lambda_1}t\right)\right) \tag{3–45}$$

and (3–42) can be used to show that $V \in \mathcal{L}_\infty$. Thus, $e_1, e_2, r \in \mathcal{L}_\infty$. Thus, from (3–12), $u \in \mathcal{L}_\infty$, which implies $u(t-\tau) \in \mathcal{L}_\infty$, and hence, $e_u \in \mathcal{L}_\infty$. The closed-loop error system can be used to conclude that the remaining signals are bounded. From (3–37) and (3–39), [69, Corollary 1] can be invoked to show that $\|\dot{z}(t)\|$ is ultimately uniformly bounded in $\mathscr{D}$ for all $y(t_0) \in \mathcal{S}_{\mathscr{D}}$. Based on the definition of z in (3–20), $\|e_1(t)\| \leq \epsilon_0 \exp(-\epsilon_1 t) + \epsilon_2$ for all $y(t_0) \in \mathcal{S}_{\mathscr{D}}$. Note that the region of attraction in (3–37) can be made arbitrarily large to include any initial conditions by increasing the control gain k_s. Furthermore, since the choice of the Filippov solution $y(t)$ was arbitrary, the result is valid for all the Filippov solutions to the closed-loop system.

3.4 Experimental Results

3.4.1 Material and Participants

The subject who participated in the study signed an informed consent corresponding to the Institutional Revision Board of the University of Florida requirements. The participant was seated in the LEM depicted in Figure 2-1A). An encoder was fixed to the leg extension machine to measure the leg angle. Stimulation was delivered by a digital stimulator to self adhesive electrode pads. Electrodes were placed over the quadriceps femoris muscle group. The pulse current amplitude and angular position signals were visible in real time and recorded on the same interface in MatLab.

3.4.2 Protocol

The experiments focused on testing the controller in (3–15), once it was adapted to the NMES, and included a time-varying input delay model, to track an angular position reference. The control gains α_1, α_2, β, and k_s were previously determined in a unique pre-trial session. To determine the performance of the delay compensator, the controller's tracking performance was compared with and without delay compensation. The subject was allowed to rest between the two sessions, to ensure a similar initial muscle state in both sessions. The two sessions differed by presence and absence of the input delay compensation in the controller: the first one did not take any delay

into account, whereas the controller used in the second session was based on the input delay compensator defined in an initial test. Both of the sessions consisted of closed-loop position tracking exercises.

Position tracking consists now in dynamic contractions. As noted in Section 3.2, the force signal that is recorded does not correspond to the same force production values as in Chapter 2. Instead of an estimation of EMD in terms of force and voltage applied as the muscle is getting fatigued, EMD is modeled as a function of time. The subject is fatigued through a closed-loop position tracking test: stimulation consists in 30 Hz electrical pulses applied to the quadriceps femoris muscle group. The desired trajectory is defined as $q_d = \sqrt{\cos^2\left(t + \frac{\pi}{2}\right)} + \sin(t)$ (see Figure 3-1).

EMD was measured at the beginning of each rise of the function, as the time lag between the onset of stimulation and the onset of the movement of limb, as depicted in Figure 3-2. The stimulation is applied during 90 seconds, thus at least 15 successive EMD values can be obtained. EMD evolution is then approximated by the function that fits the best the data points. Finally, the time-varying EMD model is implemented in the input delay RISE-based controller. The two tests were performed in the same conditions: subject and leg, muscle fatigue state, control gains, duration and stimulation parameters.

3.4.3 Results

The experimental results for closed-loop position tracking are individually depicted in Figures 3-3 and 3-4. To compare the phase differences between the two controllers, their responses are superposed in Figure 3-5. The respective errors for both controllers are plotted in Figure 3-6 Experimental data are reported in Table 3-1. The time lags corresponds, for a given value, to the time between the instant when the reference reaches that value, and the instant when the output reaches that same value. The individual time lags, over the whole experiment, for a given value are represented on Figure 3-7 for both controllers .

Finally, through the experiment, the subject described the sensation of fatigue in the stimulated muscle as increasing over the 90 seconds.

3.5 Discussion

The trajectory chosen for the tests were sufficiently fatiguing to allow compare the performance of the controllers, with and without delay compensation. During the first session, the delay was not compensated. An increased time lag between the reference and the response can be observed. The second session included a time-varying EMD model in the NMES controller, calculated from the previous session. The results in the previous section showed an important decreased response time, thus leading to a decrease of the tracking error. This study showed the value of a time-varying input delay for NMES applications.

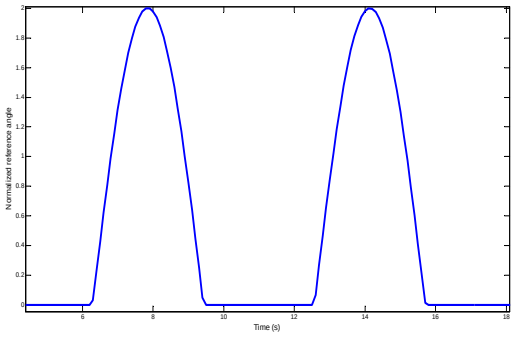

Figure 3-1. Reference input for angular position tracking

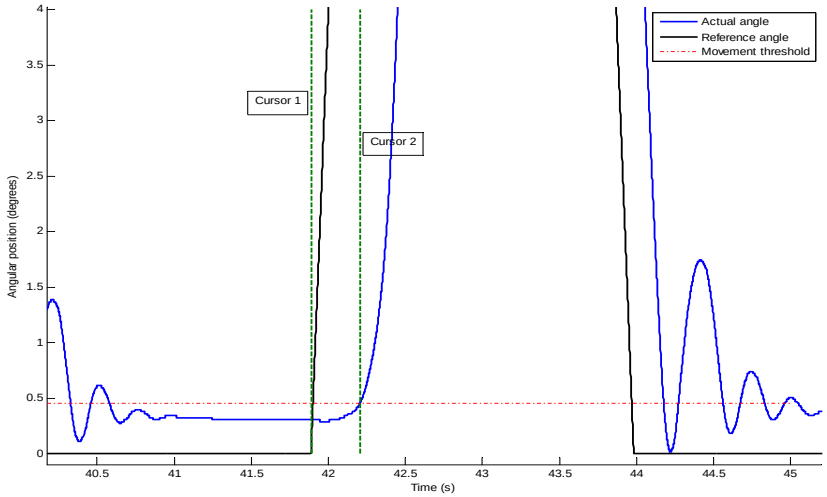

Figure 3-2. Definition of the measure of the EMD, in presence of angular position. The horizontal dashed line corresponds to the onset of the movement defined as 0.02% of the maximal output angle. The EMD is measure between the cursor 1 (onset of stimulation) and the cursor 2 (onset of movement).

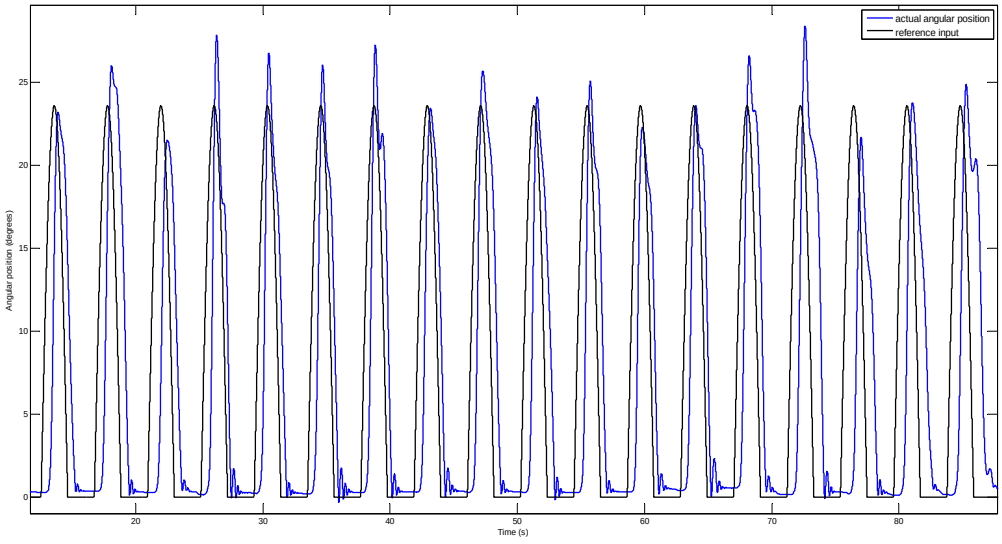

Figure 3-3. Evolution of the angular position (thick lines) during closed-loop position tracking. The controller implemented does not include any delay compensation.

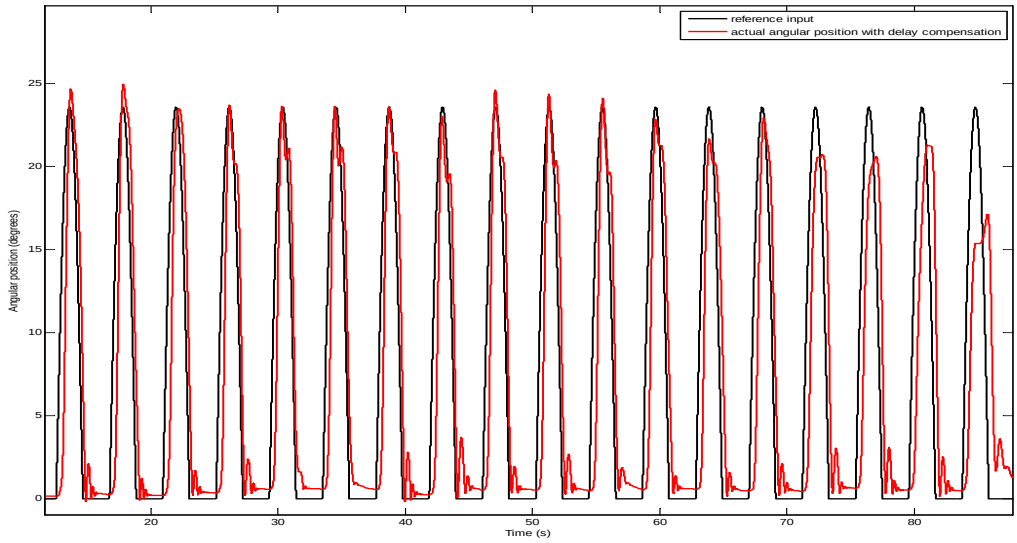

Figure 3-4. Evolution of the angular position (thick lines) during closed-loop position tracking. The controller implemented includes the time-varying model of the EMD compensation.

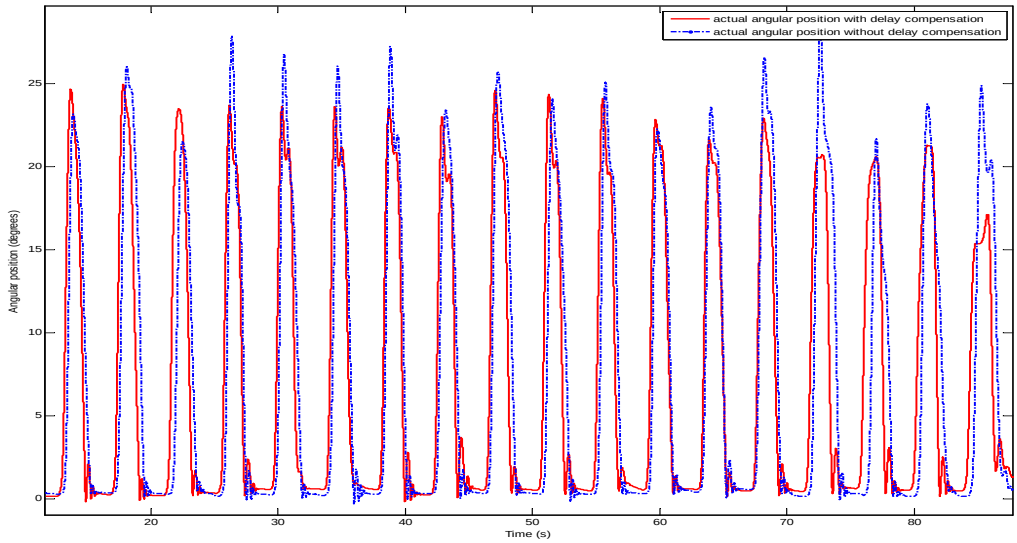

Figure 3-5. Comparison of both controllers. The dashed line corresponds to the first session, without delay compensation. The solid line corresponds to a time-varying input delay compensation controller.

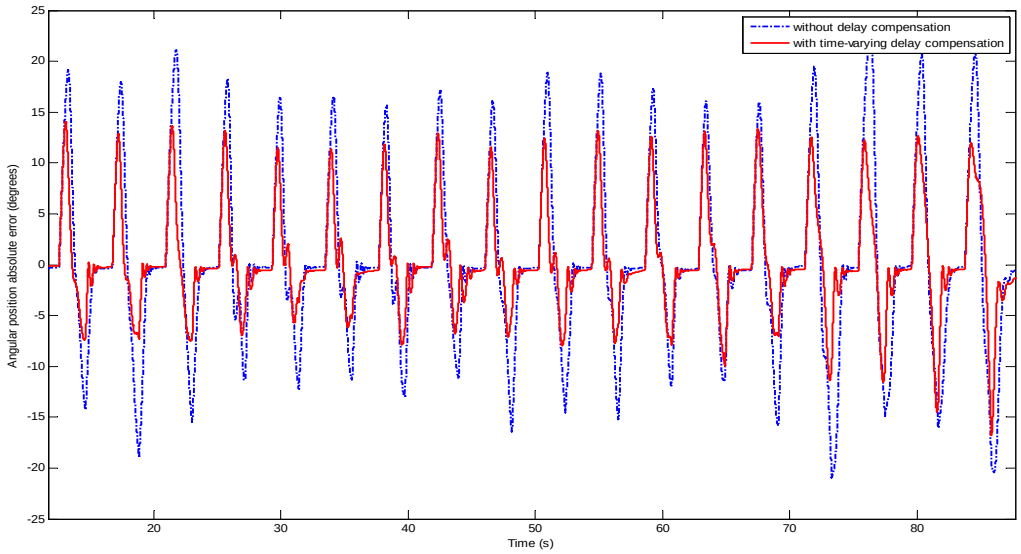

A) Tracking error

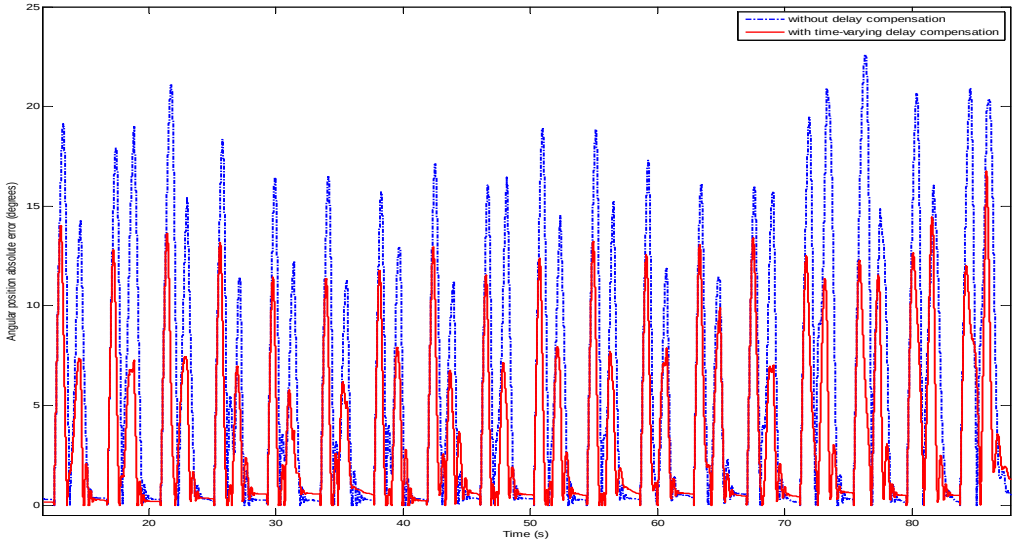

B) Absolute value of the tracking error

Figure 3-6. Evolution of the tracking error between the reference and both responses. A) Raw tracking error. B) Absolute tracking error.

Table 3-1. Experimental data for both closed-loop tracking systems

	No delay compensation	Time-varying input delay compensation
RMS error	0.0132	0.0115
Initial time lag (s)	0.535	0.498
Maximal time lag (s)	1.1	0.714

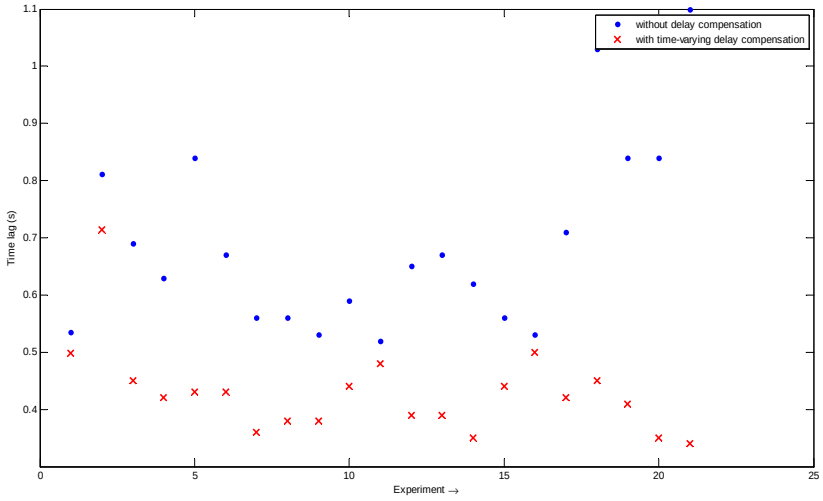

Figure 3-7. Evolution of the time lags between the reference input and the response for a given value. The blue crosses correspond to the data from the first test without delay compensation, and the red stars results from the second test with input delay compensation.

CHAPTER 4
CONCLUSION

4.1 Achievements

The objectives of the project were to prove a time, and more specifically, a fatigue dependency of the electromechanical delay during neuromuscular electrical stimulation, to model its evolution, and finally account for the time-varying input delay.

The first problem was to find a significant metric to quantify fatigue. Few trends were observable, and given the potential need to measure them during NMES control, the force produced for a certain voltage was considered as the best parameter. The main concern was the noisy signal produced by the force transducer. Filtering the signal would improve the quality of the measurements, and thus a better estimation of the EMD. However, it would also induce additional delay. To model the EMD during isometric contractions, the model in Chapter 2 includes a filtered version of the force output.

Chapter 2 described the experimental protocol for measuring the EMD. The results confirmed the assumption of the variability of the EMD with fatigue. Finally, in Chapter 3, a new time-varying EMD model was determined for dynamic contractions. A RISE-based controller was then adapted to NMES, including the compensation for the modeled input delay. Experimental results demonstrated an improved result when the time-varying input delay is compensated for.

4.2 Future Work

The research described in this thesis focused NMES in the presence of EMD. The EMD model for isometric contractions may be rendered more accurate if it is determined for a specific task. To apply this model to isometric FES control, a force tracking control has to be developed for the muscle dynamics. A challenge to develop this controller is the potential need to measure forces and derivatives of forces.

To perform FES for dynamic tasks, two EMD models may be available: a time-varying delay model, as described Chapter 3, or a fatigue-varying model. Advantages of

fatigue-varying model include the independence of the model with the task. Therefore, an EMD versus force production model should also be derived for dynamic contractions.

Next, the EMD model fits the experimental data as well as possible, but the data still contains uncertainties due to stimulation parameters or external factors, and renders the model uncertain as well. Hence, the development of an uncertain time-varying input delay compensation for nonlinear systems has to be considered.

APPENDIX
PROOF OF P

Lemma 2. *Given the differential equation in (3–32),* $P(t) \geq 0, \forall t \in [0, \infty)$ *if* β *satisfies*

$$\beta > \zeta_{N_{d1}} + \frac{\zeta_{N_{d2}}}{\alpha_2}. \tag{1}$$

For notation brevity, let $\Upsilon \in \mathbb{R}$ be defined as the integral of $\dot{P}$ in (3–32) as

$$\Upsilon = \int_{t_0}^{t} r^T(\xi)\left(N_d(\xi) - \beta sgn(\eta(\xi))\right) d\xi. \tag{2}$$

Using (3–9) and (3–10), (2) can be expanded as

$$\begin{aligned}\Upsilon = &\int_{t_0}^{t} \alpha_2 \eta^T(\xi)\left[N_d(\xi) - \beta sgn(\eta(\xi))\right] d\xi \\ &+ \int_{t_0}^{t} \frac{\partial \eta^T(\xi)}{\partial \xi} N_d(\xi)\, d\xi - \int_{t_0}^{t} \frac{\partial \eta^T(\xi)}{\partial \xi} \beta sgn(\eta(\xi))\, d\xi.\end{aligned} \tag{3}$$

Integrating the last two terms in (3) by parts yields

$$\begin{aligned}\Upsilon = &\int_{t_0}^{t} \alpha_2 \eta^T(\xi)\left[N_d(\xi) - \beta sgn(\eta(\xi))\right] d\xi + \eta^T N_d - \eta^T(t_0) N_d(t_0) \\ &- \int_{t_0}^{t} \eta^T(\xi)\left[\frac{\partial N_d(\xi)}{\partial \xi}\right] d\xi - \beta \sum_{i=1}^{n} |\eta_i| + \beta \sum_{i=1}^{n} |\eta_i(t_0)|.\end{aligned} \tag{4}$$

Based on (3–21), the expression in (4) can be upper bounded as

$$\begin{aligned}\Upsilon \leq &\int_{t_0}^{t} \alpha_2 \|\eta(\xi)\| \left[\zeta_{N_{d1}} + \frac{\zeta_{N_{d2}}}{\alpha_2} - \beta\right] d\xi \\ &+ \left\|\eta^T\right\| \left[\zeta_{N_{d1}} - \beta\right] + \beta \sum_{i=1}^{n} |\eta_i(t_0)| - \eta^T(t_0) N_d(t_0).\end{aligned} \tag{5}$$

From (5), if β satisfies the sufficient condition in (1), then

$$\Upsilon \leq \beta \sum_{i=1}^{n} |\eta_i(t_0)| - \eta^T(t_0) N_d(t_0) = P(t_0). \tag{6}$$

Integrating both sides of $P(t_0)$ in (3–32) yields

$$P = P(t_0) - \Upsilon,$$

which indicates that $P(t) \geq 0, \forall t \in [0, \infty)$ from (6).

REFERENCES

[1] V. Chaubet and T. Paillard, "Effect of unilateral knee extensor muscle fatigue induced by stimulated and voluntary contractions," *Clin. Neurophysiol.*, vol. 42, pp. 377–383, 2012.

[2] T. Paillard, J. Maître, V. Chaubet, and L. Borel, "Stimulated and voluntary fatiguing contractions of quadriceps femoris differently disturb postural control," *Neurosci. Lett.*, vol. 477, pp. 48–51, 2010.

[3] D. Jones, B. Bigland-Ritchie, and R. Edwards, "Excitation frequency and muscle fatigue: Mechanical responses during voluntary and stimulated contractions," *Exp. Neurol.*, vol. 64, pp. 401–413, 1979.

[4] S. Binder-Macleod, "Effects of activation frequency and force on low-frequency fatigue in human skeletal muscle," *J. Appl. Physiol.*, vol. 86, pp. 1337–1346, 1999.

[5] S. Binder-Macleod and L. McDermond, "Changes in the force-frequency relationship of the human quadriceps femoris muscle following electrically and voluntarily induced fatigue," *Phys. Ther.*, vol. 72, pp. 95–104, 1992.

[6] D. Sinacore, R. Jacobson, and A. Delitto, "Quadriceps femoris muscle resistance to fatigue using an electrically elicited fatigue test following intense endurance exercise training," *Phys. Ther.*, vol. 74, pp. 930–939, 1994.

[7] L. Lacourpaille, A. Nordez, and F. Hug, "Influence of stimulus intensity on electromechanical delay and its mechanisms," *J. Electromyogr. Kinesiol.*, vol. 23, pp. 51–55, 2013.

[8] S. Zhou, D. Lawson, W. Morrison, and I. Fairweather, "Electromechanical delay in isometric muscle contractions evoked by voluntary, reflex and electrical stimulation," *Eur. J. Appl. Physiol. Occup. Physiol.*, vol. 70, pp. 138–145, 1995.

[9] J. van Dieën, C. Thissen, A. van de Ven, and H. Toussaint, "The electro-mechanical delay of the erector spinae muscle: influence of rate of force development, fatigue and electrode location," *Eur. J. Appl. Physiol. Occup. Physiol.*, vol. 63, pp. 216–222, 1991.

[10] S. Yavuz, A. Sendemir-Urkmez, and K. Turker, "Effect of gender, age, fatigue and contraction level on electromechanical delay," *Clin Physiol*, vol. 121, pp. 1700–1706, 2010.

[11] S. Zhou, D. Lawson, W. Morrison, and I. Fairweather, "Electromechanical delay of knee extensors: the normal range and the effects of age and gender," *J. Hum. Mov. Stud.*, vol. 28, pp. 127–146, 1995.

[12] E. Winter and F. Brookes, "Electromechanical response times and muscle elasticity in men and women," *Eur. J. Appl. Physiol. Occup. Physiol.*, vol. 63, pp. 124–128, 1991.

[13] D. Bell and I. Jacobs, “Electro-mechanical response times and rate of force development in males and females,” *Med. Sci. Sports Exerc.*, vol. 18, pp. 31–36, 1986.

[14] S. Zhou, M. McKenna, D. Lawson, W. Morrison, and I. Fairweather, “Effects of fatigue and sprint training on electromechanical delay of knee extensor muscles,” *Eur. J. Appl. Physiol. Occup. Physiol.*, vol. 72, pp. 410–416, 1996.

[15] E. Cè, S. Rampichini, L. Agnello, A. Veicsteinas, and F. Esposito, “Effects of temperature and fatigue on the electromechanical delay components,” *Muscle Nerve*, vol. 47, pp. 566–576, 2013.

[16] K. Kubo, H. Kanehisa, M. Ito, and T. Fukunaga, “Effects of isometric training on the elasticity of human tendon structures in vivo,” *J. Appl. Physiol.*, vol. 9, pp. 26–32, 2001.

[17] P. Cavanagh and P. Komi, “Electromechanical delay in human skeletal muscle under concentric and eccentric contractions,” *Eur. J. Appl. Physiol. Occup. Physiol.*, vol. 42, pp. 159–163, 1979.

[18] M. Paasuke, J. Ereline, and H. Gapeveva, “Neuromuscular fatigue during repeated exhaustive submaximal static contractions of knee extensor muscles in endurance-trained, power-trained and untrained men,” *Acta Physiol. Scand.*, vol. 166, pp. 319–326, 1999.

[19] S. Zhou, “Acute effect of repeated maximal isometric contraction on electromechanical delay of knee extensor muscle,” *J. Electromyogr. Kinesiol.*, vol. 6, pp. 117–127, 1996.

[20] S. Binder-Macleod and T. Guerin, “Preservation of force output through progressive reduction of stimulation frequency in human quadriceps femoris muscle,” *Phys. Ther.*, vol. 70, pp. 619–625, 1990.

[21] S. Zhou, M. Carey, R. Snow, D. Lawson, and W. Morrison, “Effects of fatigue muscle and temperature on electromechanical delay,” *Electromyogr Clin Neurophysiol*, vol. 38, pp. 67–73, 1998.

[22] A. H. Vette, K. Masani, and M. R. Popovic, “Implementation of a physiologically identified PD feedback controller for regulating the active ankle torque during quiet stance,” *IEEE Trans. Neural Syst. Rehabil. Eng.*, vol. 15, no. 2, pp. 235–243, June 2007.

[23] K. Masani, A. Vette, N. Kawashima, and M. Popovic, “Neuromusculoskeletal torque-generation process has a large destabilizing effect on the control mechanism of quiet standing,” *J. Neurophysiol.*, vol. 100, no. 3, p. 1465, 2008.

[24] K. Masani, A. H. Vette, and M. R. Popovic, “Controlling balance during quiet standing: proportional and derivative controller generates preceding motor command to

body sway position observed in experiments." *Gait and Posture*, vol. 23, no. 2, pp. 164–172, Feb 2006.

[25] A. Vette, K. Masani, and M. Popovic, "Neural-mechanical feedback control scheme can generate physiological ankle torque fluctuation during quiet standing: A comparative analysis of contributing torque components," in *IEEE International Conference on Control Applications*. IEEE, 2008, pp. 660–665.

[26] N. Sharma, C. Gregory, and W. Dixon, "Predictor-based compensation for electromechanical delay during neuromuscular electrical stimulation," *IEEE Trans. Neural Syst. Rehabil. Eng.*, vol. 19, pp. 601–611, 2011.

[27] C. Minshull, N. Nigel Gleeson, M. Walters-Edwards, and D. Eston, R.; Rees, "Effects of acute fatigue on the volitional and magnetically-evoked electromechanical delay of the knee flexors in males and females," *Eur. J. Appl. Physiol.*, vol. 100, pp. 469–478, 2007.

[28] N. Sharma, C. Gregory, M. Johnson, and W. Dixon, "Closed-loop neural network-based nmes control for human limb tracking," *IEEE Trans. Control Syst. Technol.*, vol. 20, pp. 712–725, 2012.

[29] M. Krstic, *Delay compensation for Nonlinear adaptative and PDE systems*, Springer, Ed., 2009.

[30] O. Smith, "A control to overcome deadtime," *ISA J*, vol. 6, pp. 28–33, 1959.

[31] Z. Arstein, "Linear systems with delayed ccontrol: a reduction," *IEEE Trans. Automat. Contr.*, vol. 27, pp. 869–879, 1982.

[32] J. Chiasson and J. Loiseau, "Application of time delay systems," *Lecture notes in control and information sciences*, 2007.

[33] K. Gu, V. L. Kharitonov, and J. Chen, "Stability of time delay systems," *Birkhauser*, 2003.

[34] A. Manitius and A. Olbrot, "Finite spectrum assignment problem for systems with delays," *IEEE Trans. Automat. Contr.*, vol. 24, pp. 541–552, 1979.

[35] M. Jankovic, "Recursive predictor design for state and ouput feedback controllers for linear time delay systems," *Automatica*, vol. 45, pp. 510–517, 2010.

[36] ——, "Forwarding, backstepping and finite spectrum assignment for time delay systems," *Automatica*, vol. 45, pp. 2–9, 2009.

[37] N. Bekiaris-Liberis and M. Krstic, "Stabilization of linear strict feedback systems with delayed integrators," *Automatica*, vol. 46, pp. 1902–1910, 2010.

[38] M. Nihtila, "Adaptive control of a continuous time system with time-varying input delay," *IEEE Trans. Automat. Contr.*, pp. 357–364, 1989.

[39] J.-P. Richard, “Time-delay systems: an onverview of some recent advances and open problems,” *Automatica*, vol. 39, pp. 1667–1694, 2003.

[40] M. Nihtila, “Finite pole assignment for systems with time-varying input delays,” *Proceedings IEEE Conference Decision and Control*, pp. 927–928, 1991.

[41] R. Lozano, P. Castillo, P. Garcia, and A. Dzul, “Robust prediction-based control for unstable delay system: Application to the yaw control of a mini-helicopter,” *Automatica*, vol. 40, pp. 603–612, 2004.

[42] D. Yue and Q.-L. Han, “Delayed feedback control of uncertain systems with time-varying input delay,” *Automatica*, vol. 41, pp. 233–240, 2005.

[43] Z. Wang, P. Goldsmith, and D. Tan, “Improvement on robust control of uncertain systems with time-varying input delays,” *IET Control Theory Appl.*, vol. 1, pp. 189–194, 2007.

[44] M. Krstic, “Lyapunov stability of linear predictor feedback for time-varying input delay,” *IEEE Trans. Automat. Contr.*, vol. 55, pp. 554–559, 2010.

[45] H. Wu, “Adaptive robust state state observers for a class of uncertain nonlinear dydynamic systems with delayed state perturbations,” *IEEE Trans. Automat. Contr.*, vol. 54, pp. 1407–1412, 2009.

[46] S. S. Ge, F. Hong, and T. H. Lee, “Adaptive neural control of nonlinear time delay systems with unknown virtual control coefficients,” *IEEE Trans. Syst. Man Cybern.*, vol. 34, pp. 499–516, 2004.

[47] ——, “Robust adaptive control of nonlinear systems with unknown time delays,” *Proceedings of the 2004 IEEE International Symposium on Intelligent Control*, vol. 41, pp. 1181–1190, 2005.

[48] S. J. Yoo, J. B. Park, and C. H. Choi, “Adaptive dynamic surface control for stabilzation of parametric strict-feedback nonlinear systems with unknown time delays,” *IEEE Trans. Automat. Contr.*, vol. 52, pp. 2360–2365, 2007.

[49] C.-C. Hua, X.-P. Guan, and G. Feng, “Robust stabilization for a class of time delay systems with triangular structure,” *IET Control Theory Appl.*, vol. 1, pp. 875–879, 2007.

[50] M. Wang, B. Chen, and S. Zhang, “Adaptive neural tracking control of nonlinear ttime-delay systems with disturbances,” *Int. J. Adapt Control Signal Process.*, vol. 23, pp. 1031–1049, 2009.

[51] S.-C. Tong and N. Sheng, “Adaptive fuzzy observer backstepping control for a class of uncertain nonlinear systems with unknown time delay,” *Int. J. Adapt Control Signal Process.*, vol. 7, pp. 236–246, 2010.

[52] A. Kuperman and Q.-C. Zhong, “Robust control of uncertain nonlinear systems with state delays based on an uncertainty and disturbance estimator,” *Int. J. Adapt Control Signal Process.*, vol. 21, pp. 79–92, 2011.

[53] H. Huang and D. Ho, “Delay-dependent robust control of uncertain stochastic fuzzy systems with time-varying delay,” *IET Control Theory Appl.*, vol. 1, pp. 1075–1085, 2007.

[54] B. Ren, S. S. Ge, T. H. Lee, and C. Su, “Adaptive neural control for a class of nonlinear systems with uncertain hysteresis iinput and time-varying state delays,” *IEEE Trans. Neural Netw.*, vol. 20, pp. 1148–1164, 2009.

[55] S. J. Yoo and J. B. Park, “Neural-network-based decentralized adpative control for a class of large scale nonlinear systems with unknown time-varying delays,” *IEEE Trans. Syst. Man Cybern.*, vol. 39, pp. 1316–1323, 2009.

[56] M. Wang, S. S. Ge, and K. Hong, “Approximation-based adaptive tracking control of pure feedback nonlinear systems with multiple unknown time-varying delays,” *IEEE Trans. Neural Netw.*, vol. 21, pp. 1804–1816, 2010.

[57] Y. Niu, D. W. C. Ho, and J. Lam, “Robust integral sliding mode control for uncertain stochastic systems with time-varying delay,” *Automatica*, vol. 41, pp. 873–880, 2005.

[58] W. Chen, L. Jiao, J. Li, and R. Li, “Adaptive nn backstepping output-feedback control for stochastic nonlinear strict-feedback systems with time-varying delays,” *IEEE Trans. Syst. Man Cybern.*, vol. 40, pp. 939–950, 2010.

[59] B. Mirkin, P.-O. Gutman, Y. Shtessel, and C. Edwards, “Continuous decentralized mrac with sliding mode of nonlinear delayed dynamic systems,” in *IFAC World Congress, Milan, Italy*, 2011.

[60] B. Mirkin and P.-O. Gutman, “Robust adaptive output feedback tracking for a class of nonlinear tine-delayed plants,” *IEEE Trans. Automat. Contr.*, vol. 55, pp. 2418–2424, 2010.

[61] N. Fischer, R. Kamalapurkar, N. Sharma, and W. E. Dixon, “Rise-based control of an uncertain nonlinear system with time-varying state delays,” *Proceedings IEEE Conference Decision and Control*, pp. 3502–3507, 2012.

[62] N. Sharma, S. Bhasin, Q. Wang, and W. E. Dixon, “Rise-based adaptive control of a control affine uncertain nonlinear system with unknown state delays,” *IEEE Trans. Automat. Contr.*, vol. 57, pp. 255–259, 2012.

[63] I. Karafyllis, “Finite time global stabilization by means of time-varying distributed delay feedback,” *SIAM J. Contr. Optim.*, vol. 45, pp. 320–342, 2006.

[64] N. Bekiaris-Liberis and M. Krstic, “Compensation of time-varying input delay for nonlinear systems,” *Mediterranean Conference on Control and Automation, Corfu, Greece*, 2011.

[65] ——, “Compensation of time-varying input and state delays for nonlinear systems,” *J. Dyn. Syst. Meas. Contr.*, vol. 134, 2012.

[66] D. Shevitz and B. Paden, “Lyapunov stability theory of nonsmooth systems,” *IEEE Trans. Autom. Control*, vol. 39 no. 9, pp. 1910–1914, 1994.

[67] B. Paden and S. Sastry, “A calculus for computing Filippov’s differential inclusion with application to the variable structure control of robot manipulators,” *IEEE Trans. Circuits Syst.*, vol. 34 no. 1, pp. 73–82, 1987.

[68] F. H. Clarke, *Optimization and nonsmooth analysis*. SIAM, 1990.

[69] N. Fischer, R. Kamalapurkar, and W. E. Dixon, “Lasalle-yoshizawa corollaries for nonsmooth systems,” *IEEE Trans. Automat. Control, to appear (see also arXiv:1205.6765v2)*, to appear.

BIOGRAPHICAL SKETCH

Fanny Bouillon was born in France, where she received her French Baccalaureat in the scientific section in 2008. After two years in mathematics, physics and engineering sciences preparatory classes for higher education schools, she entered the engineering program in Télécom Physique Strasbourg. The Atlantis CRISP Dual Degree international exchange program allowed her to complete the third year at the University of Florida in the US, in the Nonlinear Controls and Robotics group, working on neuromuscular electrical stimulation, under the advisement of Dr. Warren Dixon.